Instituto Tecnológico y de Estudios Superiores de Monterrey

Campus Monterrey

School of Engineering and Sciences

POLYETHYLENE ENGINEERING FOR APPLICATION IN PASSIVE PERSONAL THERMAL MANAGEMENT

A thesis presented by

Jesús Eduardo Ramos Tirado

Advisor:

Dr. Alan Osiris Sustaita Narváez

Co-Advisor:

Luis Marcelo Lozano Sánchez

Submitted to the

School of Engineering and Sciences

In partial fulfillment of the requirements for the degree of

Master of Science in

Nanotechnology

Monterrey, Nuevo León, December 2021

Acknowledgements

I would like to express my deepest gratitude to my advisors Alan Sustaita and Marcelo Lozano, they fuide me through all this journey developing my masters project in a short time due the pandemic situation.

I would also like to thank my lab mates to give me ideas and support me during my experiments to get the job done.

Finally, I would like to thank the Tecnológico de Monterrey for it support on tuition and CONACyT with the support for living.

"POLYETHYLENE ENGINEERING FOR APPLICATION IN PASSIVE PERSONAL THERMAL MANAGEMENT"

By

Jesús Eduardo Ramos Tirado

Abstract

Thermal comfort is the mind condition when we feel satisfaction with the environmental conditions. Thermoregulatory clothing is an energy-saving way to achieve thermal comfort conditions. Lately, there have been efforts to develop materials with thermoregulatory properties. The simple structure of polyethylene makes a good option for engineering thermoregulatory fibers due to its transparency windows in the mid-IR, where we emit radiation to the environment. In this project, it is proposed an alternative method to fabricate oriented UHMWPE films with high crystallinity and high fibers and molecular chains orientation to enhance the thermal conductivity of the films. The restructuring of the films was measured using FTIR/ATR Spectroscopy, DSC, XRD, SWAXS and SEM. The films obtained show an increase in crystallinity and chains orientation as the draw ratio increase, which leads to a higher thermal conductivity.

List of figures

Figure 1. Heat loss rates of human body at different temperatures [12] (Replicated illustrative graph). 4
Figure 2. Percent Energy Savings in different cities in the US obtained by Hoyt et al [8]. (Replicated illustrative graph)..... 6
Figure 3. **a)** Measured total FTIR transmittance of nanoporous PE (nanoPE), normal PE, and cotton. Because of the small pore size, nanoPE is as transparent as normal PE. Cotton, on the other hand, is completely opaque. Human body radiation is indicated by the yellow shaded region. **(b)** FTIR total transmittance spectra of common textiles. NanoPE is also shown for comparison. (Adapted only for illustrative purposes from [9]). 11
Figure 4. Schematic of dual-mode textile. (A) Traditional textiles only have single emissivity, so the radiation heat transfer coefficient is fixed. (B) For a bilayer thermal emitter embedded in the IR-transparent nanoPE, when the high-emissivity layer faces outside and the nanoPE between the skin and the emitter is thin, the high emissivity and high emitter temperature results in large heat transfer coefficient, so the textile is in cooling mode. (C) The textile is flipped, and the low emissivity and low emitter temperature cause the heat transfer coefficient to decrease. The textile now works in heating mode [37]. 12
Figure 5. Transmittance of Ultra High Molecular Weight Polyethylene (UHMWPE) film. Mid-infrared transparency window of polyethylene overlaps with the atmospheric transparency window (green range) which coincide with the human body radiation emitted (blue curve), enabling the use of polyethylene in radiative cooling. 13
Figure 6. Illustration of UHMWPE powder crystallites embedded in a disordered and entangled chain network. 15
Figure 7. Test tubes for stretching. The blue zone is the part held by the jaws of the universal testing machine, while the white zone is the stretch zone of the film. 16
Figure 8. Representation of drawns of each film a, в, and г, before a fracture a) along to and в) perpendicular to draw axis. The black dot points in film в represents outlier data in that film..... 19
Figure 9. FTIR/ATR spectrum of UHMWPE powder. 20
Figure 10. Transparency window of UHMWPE x0 with respect to the human body radiation and the transparency window measured by FTIR/ATR. 21
Figure 11. Themogram of UHMWPE x0 and x50 films and other materials to demonstrate the IR transparency of UHMWPE films. 21
Figure 12. FTIR/ATR spectrum stacking of UHMWPE powder and films x0, x50 and x100..... 22
Figure 13. Comparison on bending deformation absorption bands in UHMWPE Powder, and x0, x50 and x100 films. 23
Figure 14. Comparison on rocking deformation absorption bands in UHMWPE Powder, and x0, x50 and x100 films. 23
Figure 15. X-Ray diffractogram of UHMWPE film x0, x50 and x100. 24
Figure 16. First heat thermogram's DSC of UHMWPE powder sample and film x0, x50 and x100 samples..... 26
Figure 17. SEM images of UHMWPE films a) x0, в) x50 and c) x100 and WAXS 2D diffracograms patterns obtained from UHMWPE films d) x0 and e) x100, which demonstrate the alignment of the fibers (SEM) and crystallites (WAXS) along the draw axis. 27
Figure 18. Schematic representation of an undrawn films and the restructuration of the film after the draw process. The aligment of the crystals and fibers along the stretch axis increase. 28
Figure 19. Prototype of thermal conductivity characterization. a) Is the back view of vacuum chamber (visible window with the collimator), в) is an isometric view of the vacuum chamber it can be appreciated the thermal resistor at the top of the chamber, c) is the front view of the vacuum chamber (infrared window). d) Schematic representation of the design of the thermal measurement arrengment..... 29

List of Tables

TABLE 1. RESULTS OF THE FIVE-TEST SPECIMEN OF EACH FILM (A, B, AND Г) BEFORE A FRACTURE ALONG TO AND PERPENDICULAR TO DRAW AXIS, THEY MEAN AND STANDARD DEVIATION. THE MISSING DATA IN **AE** IS DUE TO IT FRACTURED PERPENDICULAR TO THE DRAW AXIS IN THE X37 RATIO, SO THIS TEST SPECIMEN WAS NOT CONSIDERED FOR ANY MEAN OF FILM **A**. 19
TABLE 2. VARIATION OF CRYSTALLINITY IN UHMWPE FILMS WITH DIFFERENT DRAW RATIOS BY FTIR. 24
TABLE 3. DEGREE OF CRYSTALLINITY CALCULATED FROM X-RAY DIFFRACTOGRAM. 25
TABLE 4. DEGREE OF CRYSTALLINITY CALCULATED FROM DSC..... 25
TABLE 5. RESULTS OF CRYSTALLINITY FROM FTIR-ATR, XRD AND DSC. 26
TABLE 5. RESULTS OF CRYSTALLINITY FROM FTIR-ATR, XRD AND DSC. 28

Table of Contents

LIST OF FIGURES VI

LIST OF TABLES VII

1. INTRODUCTION 1

2. HYPOTHESIS AND OBJECTIVES 3

2.1. HYPOTHESIS 3
2.2. GENERAL OBJECTIVE 3
2.3. SPECIFIC OBJECTIVE 3

3. STATE OF ART 4

3.1. HUMAN THERMOREGULATION 4
3.2. THERMAL COMFORT 5
3.3. CLOTHING WITH THERMOREGULATORY PROPERTIES 7
3.3.1. Active Thermoregulatory Clothing (ATC) *7*
3.3.2. Passive Thermoregulatory Clothing (PTC) *8*
3.3.2.1. Phase Changing materials 8
3.3.2.2. Moisture responsive fabrics 9
3.3.2.3. Radiative transparent/reflective textiles 9
3.4. POLYETHYLENE IN THERMOREGULATORY APPLICATIONS 13
3.4.1. Passive radiative cooling of buildings *14*
3.4.2. Personal passive radiative cooling *14*
3.4.3. Metal-like conductor *15*

4. MATERIAL AND METHODS 16

4.1. MATERIALS 16
4.2. POLYETHYLENE FILMS 16
4.3. FOURIER-TRANSFORM INFRARED SPECTROSCOPY (FTIR) 17
4.4. X-RAY DIFFRACTION (XRD) 17
4.5. DIFFERENTIAL SCANNING CALORIMETRY (DSC) 17
4.6. SCANNING ELECTRONIC MICROSCOPY (SEM) 18
4.7. SMALL AND WIDE-ANGLE X-RAY SCATTERING (SWAXS) *IN PROGRESS* 18

5. RESULTS AND DISCUSSION 19

5.1. POLYETHYLENE FILMS FABRICATION 19
5.2. CHARACTERIZATION OF THE FILMS 20

6. FUTURE WORK 29

7. CONCLUSIONS 31

8. REFERENCES 32

APPENDIX A. FTIR SPECTRUMS OF UHMWPE FILMS 38

APPENDIX B. SCIENTIFIC DISSEMINATION ARTICLE PUBLISHED IN TRANSFERENCIATEC JOURNAL 39

1. INTRODUCTION

Thermal comfort is a mind condition that makes the user feel satisfaction with the environment and its thermal conditions. The American Society of Heating, Refrigerating and Air Conditioning Engineers (ASHRAE) has defined the physiological and environmental conditions to achieve thermal comfort [1]–[4]. The human body has two main mechanisms to heat exchange with the environment to achieve thermal homeostasis: evaporative and no evaporative heat loss.The contribution of the different mechanisms will depend on the difference in temperatures between the body and its environment; the two main ways of heat exchange will be evaporation and radiation. Nevertheless, in some environments, the thermoregulatory mechanism of the body is not enough to achieve thermal comfort. Therefore clothing and HVAC (Heating, Ventilation, and Air Conditioning) systems were developed to help the body thermoregulates depending on the environmental conditions [5]. The problem with the HVAC systems is its energy consumption which is between 20-40% [6], [7]. This problem can be solved by engineering materials to directly manage the heating and/or cooling on humans by Personal Environmental Control (PEC) systems [8], leading to energy saving and energy efficiency called "Personal Thermal Management".

Clothing with thermoregulatory properties is the PEC system most used. It can be divided into Active (ATC) and Passive (PTC) Thermoregulatory Clothing. The first one needs some external work as a power supply to active the thermoregulatory system, while the passive kind depends only on the material properties for thermoregulation. Lately, there have been many efforts to develop flexible, lightweight, breathable, and intelligent textile materials to enhance thermal comfort.

As mentioned before the radiation is one of the main ways of heat exchange to thermoregulates the human body temperature. The human skin has emissivity ≈0.98, which makes it an excellent emitter in the mid-infrared range [9]. A theoretical Infrared-Transparent Visible-Opaque Fabric (ITVOF) has been proposed by Tong et al. [10], which would provide passive cooling transmitting the thermal radiation emitted by the human body to the environment. The authors demonstrated that a fabric composed of parallel-aligned polyethylene (PE) fibers could achieve the requirements of an ITVOF. The simple structure of this polymer gives a low absorptance in the visible, near- and mid-IR spectra, but the use of PE fibers as a textile material can be a problem because it is visibly transparent to the human eye and does not have the common textile properties as air permeability and water-wicking. Engineering can be applied to PE to reflect sunlight while keeps its mid-IR transparency properties, which can be achieved fabricating PE fibers with diameters equivalent to the wavelength of solar radiation or embedding pores in PE fibers leading to the same effect.

Not only the optic properties can be engineered to make PE fibers a potential thermoregulatory textile material, most thermoplastic polymers (just as polyethylene) are poor heat conductors, due it partially crystalline and partially amorphous structure. However, carbon-based materials are potentially the best heat conductors, the fact that PE is a backbone C-C. It has been demonstrated that highly crystalline and stretched polyethylene films and fibers, with oriented polymer chains, provide high thermal conductivity and superior mechanical properties [11]–[19]. This enhancement in thermal conductivity can be used to remove heat from hot spots in the body.

In this project, the focus is to propose an alternative method to fabricate ultra-oriented polyethylene films from that reported by Loomis et al [11], which consist in dissolution of Ultra High Molecular Weight Polyethylene (UHMWPE) in decalin and casted onto liquid-nitrogen cooled substrates to obtain films and then draw them in a 90°C heated roll-to-roll system. The alternative that is proposed in this project is a substrate cooled at -8°C in a cooler instead with liquid-nitrogen and a uniaxial drawing system with convection heat at 38°C. The mechanical tension applied will restructure the material orienting its chains and fibers, leading to high crystallinity and ultra-oriented polyethylene films with optical and thermal properties to apply in thermal management devices or textiles. The restructuring of the material, their degree of crystallization, orientation and transparency window in the mid-IR is measured using FTIR, DSC, XRD, SWAXS and SEM. A restructuring with an increase in crystallization and orientation and mid-IR transparency preservation were achieved which suggest a thermal conductivity and an potential material to be applied in thermal management.

2. HYPOTHESIS AND OBJECTIVES

2.1. Hypothesis

It is possible to obtain a polymer film of UHMWPE with high thermal conductivity by orienting its chains through an uniaxial drawing process.

2.2. General Objective

To perform molecular engineering to ultra-oriented UHMWPE films with an alternative manufacturing method that the reported in literature to achieve thermal conductivity due chain/internal fibers alignment and increase in crystallinity.

2.3. Specific Objective

- Establish an alternative to fabricate and stretch UHWMPE films, maintaining their optical and thermal properties.
- Stretch the films to similar draw ratios reported in the literature.
- Determine the conservation of the optical (in the mid-infrared) and thermal properties of the films using an alternative method of synthesis and drawing.

3. STATE OF ART

3.1. Human Thermoregulation

The human body is a thermo-regulated organism, which means that it maintains its temperature within a certain range via internal processes while still being responsive to environmental stimuli. There are two mechanisms of heat exchange within the human body and its environment: evaporative heat loss (sweat evaporation) and non-evaporative heat exchange (via convection, conduction, and radiation).

Thermal conduction occurs between two objects in contact with a temperature gradient—the heat transfers from the high-temperature object to the low-temperature one. Thermal convection occurs in the atmosphere, and it is the flow of a fluid by different densities due to temperature. Thermal radiation is electromagnetic radiation generated by matter objects with temperatures above absolute zero.

The way the heat produced by the body dissipates to the environment will depend on the temperature gradient between the body and its environment. The human body temperature is generally higher than its environment temperature, so most of the heat produced by the body is lost through radiation, conduction, or convection, and also by evaporation at high temperatures.

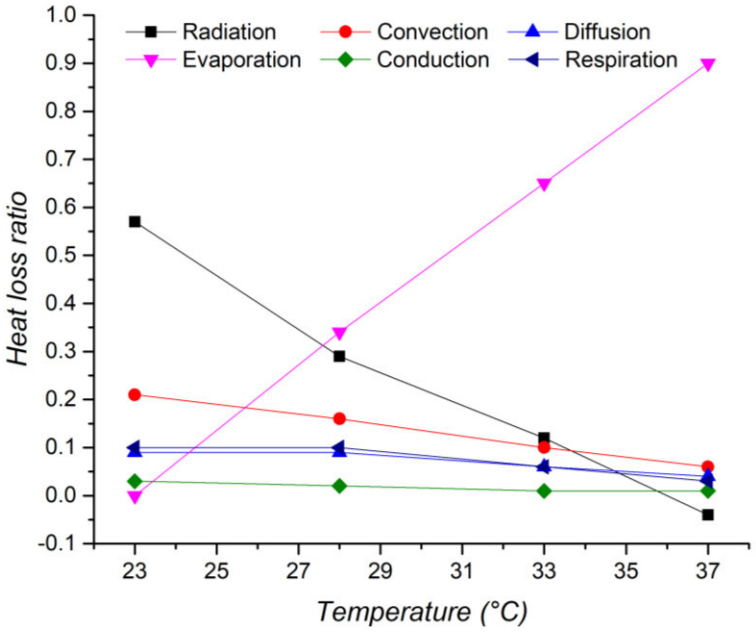

Figure 1. Heat loss rates of human body at different temperatures [12] *(Replicated illustrative graph).*

At ambient temperature, radiation and convection are the most significant mechanisms of heat loss, representing approximately 75% of heat loss. Evaporation is the

next major source accounting for 22%, and conduction represents a minor part (3%). When the temperature rises, radiation and convection heat losses rates decrease, while the evaporation heat loss increases. Conduction heat loss remains almost constant [12].

In hot conditions, the body will maximize heat loss by different mechanisms, including evaporative cooling and highly vascularized extremities. To retain heat in cold environments, vascular countercurrent exchange systems mitigate heat escaping through the extremities by transferring heat from outgoing arterial to incoming venous blood. Metabolic adaptation includes the ability to store metabolic energy in the form of fat. Through thermogenesis, energy can be released rapidly or gradually [13].

However, the skin temperature changes rapidly under most environmental conditions, and the thermoregulation mechanisms could fail thusresulting in discomfort, physiological damage, metabolic alterations or, in extreme cases, death. Therefore, clothing was developed to achieve "thermal comfort" by keeping people warm in cold conditions and blocking the heat from the environment in hot conditions.

3.2. Thermal Comfort

According to the American Society of Heating, Refrigerating and Air-Conditioning Engineers (ASHRAE), thermal comfort is the condition of mind that expresses satisfaction with the thermal environment and is assessed by subjective evaluation. The physiological conditions for a neutral thermoregulation are a core temperature of 36.6°C-37.1°C, mean skin temperature of 33°C-34.5°C in men and 32.5°C-35°C in women, not sweating (to cool) and not shivering (to warm), and dry skin with only insensible perspiration; to get keep this physiological conditions the ambient temperature must be 28°C-30°C with naked skin, but since thermal comfort also depends on psychological factors and sensations aspects the comfort zone would be in the range of 23°C-26°C, for most people, with light clothing and relative humidity of approximately 50% according to different studies [1]–[4].

When the ambient temperature is below or above the "comfort zone" (23°C-26°C) a HVAC (Heating, ventilation, and Air Conditioning) system can be used to provide the environmental requirements of the comfort of occupants in a building [5]. But a large amount of energy is consumed by HVAC systems to maintain control of air temperature in buildings [6] which has already raised concerns in heavy environmental impacts (global warming, climate change, etc.). The global contribution of buildings with HVAC systems (residential and commercial) in energy consumption figures between 20% and 40% [7]. A way to solve this energy consumption is through the constructions of energy-efficient buildings based on improving insulation and design. However, there is still a large portion

of energy wasted to maintain the temperature of empty space and inanimate objects inside the building rather than focusing on humans. But if heating and cooling could be managed directly based on humans by a personal environmental control (PEC) system, a vast amount of energy could be saved, because a human body has much less thermal mass as compared with an entire building, which results in energy saving, this energy-efficiency approach is called "Personal Thermal Management".

A PEC system could help to increase the cooling setpoint and decrease the heating setpoint. Hoyt et al. (2005) [6] simulated the energy savings possible from modifying the heating and cooling setpoints for different locations in the US. When the cooling setpoint is increased by one degree from 24°C to 25°C results in energy savings of 7-15%. In the other case, if the heating setpoint is decreased by one degree from 21.5°C to 20.5°C results in energy savings of 7-14%.

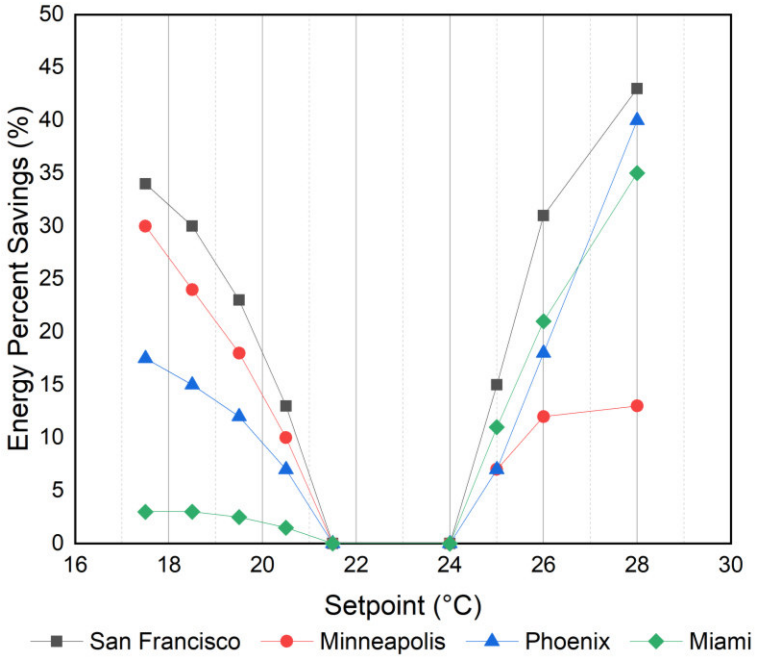

Figure 2. Percent Energy Savings in different cities in the US obtained by Hoyt et al [8]. *(Replicated illustrative graph).*

The best way to develop a PEC is by clothing, we have always been inspired to mimic nature to create our clothing materials with higher levels of functionality and smartness to achieve the thermal comfort. The ideal fabric would be like skin, which a very smart material. The skin has sensors that detect changes in temperature, which together with our brain it responds to different stimulus to maintain the normal physiological conditions, like generating sweat to cool when it is hot, stimulate blood circulation when it is cold, color change when exposed to high levels of sunlight, etc. However, normal clothes and most

textiles have limited range of sensorial properties, which usually fails to keep thermal comfort in environments with fluctuating weather.

3.3. Clothing with Thermoregulatory Properties

Lately, there have been many efforts to develop thermoregulatory clothing to enhance the thermal comfort in ambient conditions or to achieve at least physiological conditions in extreme weathers.

Heat conservation, in winter conditions, can be achieved by adding insulation or heating elements into clothing, but ensuring breathability and avoid bulk and weighted clothes. Using traditional clothes, increasing the number of layers of clothes will let to block heat loss from the body, but this leads to bulky clothes.

For cooling, according to the rates of heat loss mechanisms [12], at ambient temperature it would be needed clothes with similar skin emissivity for indoor conditions, and breathability to allow convection heat loss, and at higher temperatures clothes with high moisture wicking rates to allow heat loss by evaporation. In this case almost all the traditional clothes fail in the interaction with the radiation emitted by human body and block the evaporation of sweat.

Thermoregulatory clothing can be divided in two categories: active thermoregulatory clothing (ATC) and passive thermoregulatory clothing (PTC). The firs kind will need some external work to activate the mechanism which allows the thermoregulation, while in passive thermoregulatory, the mechanism is always activated since it depends on the material properties.

3.3.1. Active Thermoregulatory Clothing (ATC)

Textiles with thermoregulatory wearable equipment can improve thermal comfort with different approaches, some of them are the variable thermal insulation materials, managing thermal convection by fluid flow heating/cooling or thermoelectric air cooling/heating. This kind of thermal management can be achieved using a power supply for the thermoregulatory wearable equipment.

The most common approach to develop an ATC is managing thermal convection by the addition of some rigid equipment like fans or vortex tube air conditioners, this leads to manipulate the microclimate conditions (environment between human skin and clothes). Battery fans added to normal clothes can cause airflow exchange between environment and the microclimate leading to personal cooling [14], [15].

Thermal radiation can also be managed by ATC with portable power supply. Thermoelectric materials can create heat flux and produce heating/cooling based on Peltier effect between junctions of different materials, Zhang et al [16], [17] reported a thermoelectric clothing by thermally sealing high-quality inorganic TE micro/nanowires in the polymeric fibers, which achieve a 5°C cooling as maximum. For heating, a power supply can be used to emit thermal radiation based on Joule mechanism, using metallic materials embedded in normal clothes for heating clothes in winter, materials like silver, copper, graphene, etc. are mixed as nanoparticles or nanowires with fibers to produce heating because their excellent electrical conductivity [18]–[20].

The use of ATC is very effective in thermal management to achieve desired conditions to improve thermal comfort, but the addition of some rigid equipment (fans) can be uncomfortable for wearer, and the mix of normal fiber with metallic nanowires can affect breathability and softness properties of textiles, which leads to uncomfortable clothes in the day to day.

3.3.2. Passive Thermoregulatory Clothing (PTC)

Advanced materials and structures can control heat transfer between the human body and environment by the mechanisms which thermoregulation occurs (conduction, convection, radiation, evaporation). The overall advantage of PTC versus ATC is the fact that the first one does not use power supply to achieve thermal comfort modifying the thermal setpoint for cooling/heating, which leads to energy saving.

Lately, many efforts have been done to develop thermal management textiles with different properties to enhance the thermal comfort, like flexibility, lightweight, breathable, and adaptive to different environmental changes.

3.3.2.1. *Phase Changing materials*

Phase Change Materials (PCMs) are latent heat-storage materials, they can store heat energy in a high temperature environment through phase change while the temperature of the PCMs does not change much. PCMs latent heat storage can be achieved through solid-solid, solid-liquid, solid-gas, and liquid-gas phase change. But the only phase change for PCMs in textiles is the solid-liquid, because the gas phase uses a large volume or have high pressures, and the solid-solid phase change are very slow [21]. Some of PCMs which have been used to prepare thermoregulatory clothing are paraffin waxes, salt hydrates and fatty acids [22].

Some techniques to incorporate PCMs in textiles are coating or encapsulation to make thermo-regulated textiles [23]. Another way to incorporate PCMs is packing them into small bags an put in pockets or stitched in a vest [24], but this is inconvenient, heavy, and very short-term duration. To avoid these problems, the encapsulation method is used,

where the PCMs are encapsulated in the fibers or microcapsules, minimizing its usage, and obtaining a uniform dispersion of the PCM to manage heat transfer [25].

3.3.2.2. Moisture responsive fabrics

The active muscles movement lead to a high rate of perspiration, which leads to an uncomfortable sensation of wet clothes. Moisture transport of textiles is affected by wicking and evaporation rate. Fabrics with higher surface areas improves evaporation rates with faster moisture wicking [26], [27]. These smart fabrics transport the moisture and sweat from skin's wearer to the fabric surface, and it is released to the environment.

To achieve a greater surface area in a fabric, microfibers have been proposed to use over other normal fibers, as the fiber size is decreased, the surface area of yarn increases, which leads to a greater number of pores, which allow better rates of vapor transportation. Another advantage of microfibers is lightweight, comfortable and softness [28].

Some approaches to improve moisture wicking in fabrics are the use of plasma technology [29], functional sportswear with hydrophobic outer and hydrophilic inner sides, plasma treatment to monolayer fabrics with hydrophobic/hydrophilic properties [30], dual layer textiles have great potential with higher rates of moisture transfer [31]. Electrospun nanofibers are also used to modify normal textiles to improve their moisture wicking, Dong et al. [32] reported electrospun non-woven mats with good moisture transfer properties using a thick hydrophilic layer of polyacrylonitrite nanofibers with a hydrophobic polystyrene nanofibers thin layer coated with polydopamine.

3.3.2.3. Radiative transparent/reflective textiles

The human skin is an excellent IR emitter, with emissivity ≈0.98. At normal skin temperature (32-34.5 °C), the human body emits radiation in the mid-infrared range, between 7 and 14 μm, with a peak emission at 9.5 μm [9]. Since IR radiation heat loss in humans contributes more than 50% to the total body heat loss, focus on this mechanism to achieve thermal comfort must be an effective way of personal thermal management. Thermal Radiation Management has shown effective ways of heating and cooling materials for textiles applications [9], [18], [33]–[39].

Many species living in an extreme environment have shown capacity to adapt and survive. If adaptation mechanisms of these species are implemented in the design of new materials, the thermal control near the human body could be reached. This field of study embracing the practical use of mechanisms and functions of biological science in engineering, and other sciences is called Biomimetic [40]. For example, Saharan silver ants have the capacity to live under extreme temperature conditions due to their dense array of triangular hairs with two thermoregulatory effects, the first one is the reflectivity of the ant's body surface in the visible and near infrared spectrum, where solar radiation

culminates. The second thermoregulatory effect is the emissivity of the mid-infrared radiation emitted by the ant's body keeping them cool [32]. Polar bears have shown amazing capabilities to live in extremely cold environments and keeping warm, this mechanism is due to their hollow hairs that effectively reflect infrared emission from their bodies keeping the heat near of them [41]. Leung et al [41] reported a composite material with tunable thermoregulatory properties by leveraging the static infrared-reflecting design of the space blanket and drawing inspiration from the dynamic color-changing ability of squid skin.

For personal cooling in hot weather, it is necessary a textile transparent in the mid-IR range but opaque in visible range. An IR-transparent textile would allow for cooling set-points to be higher. Polyolefin films that have an IR-transmittance of 95% require a setpoint of 25.8°C, whereas IR-opaque materials such as cotton textile require a setpoint of 22.6°C, roughly 3°C lower. Song et al [36] proposed a tri-layered structure of nylon, polyvinylidene fluoride and polyethylene for personal cooling, this composite textile decreased the human body temperature by 4.5-6.5 °C under direct sunlight.

Tong et al [10] proposed a theoretical Infrared-Transparent Visible-Opaque Fabric (ITVOF), which provides passive cooling via the transmission of thermal radiation emitted by the human body directly to the environment. It was found that his fabric requires a minimum IR transmittance of 0.644 and a maximum IR reflectance of 0.2 to ensure thermal comfort at high (26.1°C) ambient temperatures. These requirements were also achieved by a fabric composed of parallel-aligned polyethylene fibers with 1 μm diameter bundled into 30 μm yarns which show an IR transmittance of 0.972 (very similar to human body emissivity). The fabrication of an ITVOF could be achieved with conventional manufacturing processes like drawing, extrusion, or electrospinning.

The challenge for developing an ITVOF is that the radiation spectrum (7-14 μm) overlaps with most of the IR absorption wavelength of common textile material, for example: C–O stretching (7.7-10 μm), C–N stretching (8.2-9.8 μm), aromatic C–H bending (7.8-14.5 μm), S=O stretching (9.4-9.8 μm), and others. As a result, most textile materials strongly absorb human body radiation and have very low IR transparency. Polyolefins such as PE have only aliphatic C–C and C–H bonds and consequently have narrow absorption peaks centered at the wavelengths of 3.4, 3.5, 6.8, 7.3, and 13.7 μm [9], which are all far away from the peak of human body radiation. However, one cannot use a normal PE film as textile material because it is visibly transparent and does not have desired properties for textile, such as air permeability and water-wicking.

Hsu et al. [9] in 2016 proposed nanoporous polyethylene as an ITVOF, its pore size distribution (50 to 1000 nm) made this material opaque to human eye, but it was not

enough to achieve the desired textile properties (air permeability and water wicking). To improve air permeability nanoPE was punched using microneedles creating 100 µm holes spaced 500 µm apart; this punched nanoPE was coated with hydrophilic polydopamine (PDA) to enhance fluid wicking, and then a cotton mesh was sandwiched by two layers of PDA-nanoPE and bonded with point welding, this reinforced the mechanical strength. They demonstrated that nanoPE is a favorable material to design human cloth for personal thermal management with some modifications to enhance its textile properties.

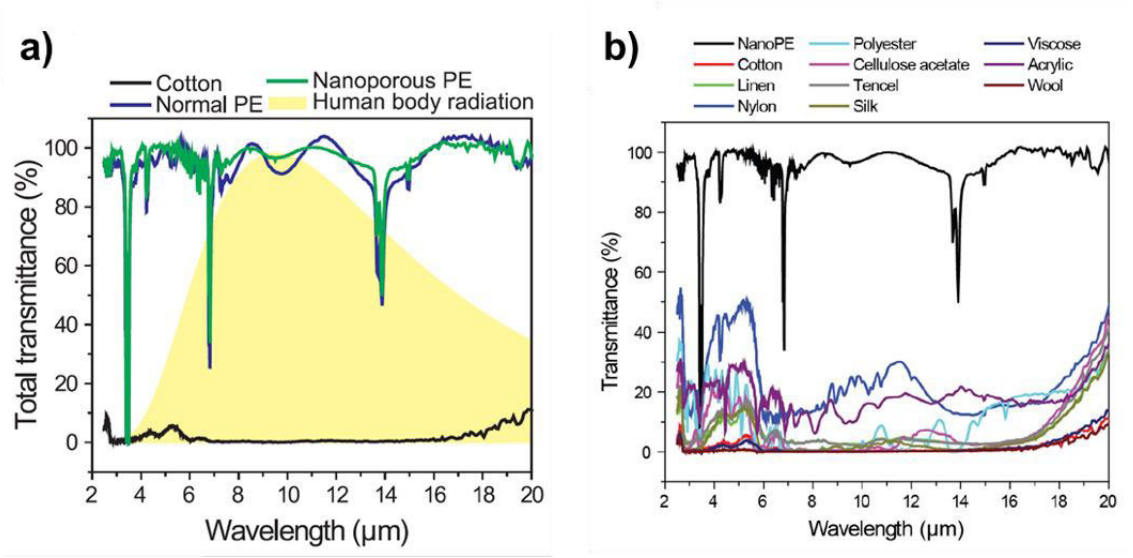

Figure 3. ***a)*** *Measured total FTIR transmittance of nanoporous PE (nanoPE), normal PE, and cotton. Because of the small pore size, nanoPE is as transparent as normal PE. Cotton, on the other hand, is completely opaque. Human body radiation is indicated by the yellow shaded region.* ***(b)*** *FTIR total transmittance spectra of common textiles. NanoPE is also shown for comparison. (Adapted only for illustrative purposes from* [9]*).*

For heating in cold weather, the IR radiation emitted by the body should be reflected toward the body to keep the microclimate between human skin and clothes warm. Hsu et al [38] reported a system thermal management material using metallic nanowire-embedded cloth that can reduce this waste. The metallic nanowires form a conductive network that not only is highly thermal insulating because it reflects human body infrared radiation but also allows Joule heating to complement the passive insulation, here the active and passive mechanism to achieve thermal comfort appears in the same material. Cai et al [39] demonstrated a nanophotonic structure textile using nanoporous metallized polyethylene, this material achieves a very low emissivity of 10.1% on the outer side that suppresses heat loss by radiation without sacrificing wearing comfort, this properties make possible decrease of the set-point in 7.1 °C compared to common textiles.

Lately there have been some efforts to achieve a dual-mode thermal radiation material (cooling and heating) for personal thermal management, which represents a

challenge to achieve since heating and cooling are opposite functions. Yue et al. [42], developed a multifunctional Janus Cu/MnO_2/cellulose@Layered Double Hydroxide fiber (CMCFL) membrane with sandwich structure fabricated by vacuum filtrating ultralong MnO_2 nanowires and Cu nanowires sequentially on cellulose fiber@Layered Double Hydroxide (LDH) basement membrane, this membrane shows asymmetrical characteristics of infrared radiation emissivity: the Cu nanowires layer (low-emissivity) is facing outside to reduce the thermal radiation to the environment, and the cellulose@LDH layer (high emissivity) is facing to the environment to enhance the heat dissipation.

Hsu et al. [37] obtained a dual-mode textile composed by a bilayer emitter embedded inside and nanoporous polyethylene (nanoPE) layer, the asymmetrical emissivity and thickness of nanoPE layer resulted in two different heat transfer coefficients when the high emissivity layer is faced to the environment the cooling mode is activated, and when the low emissivity layer is faced to outside the heating mode is on.

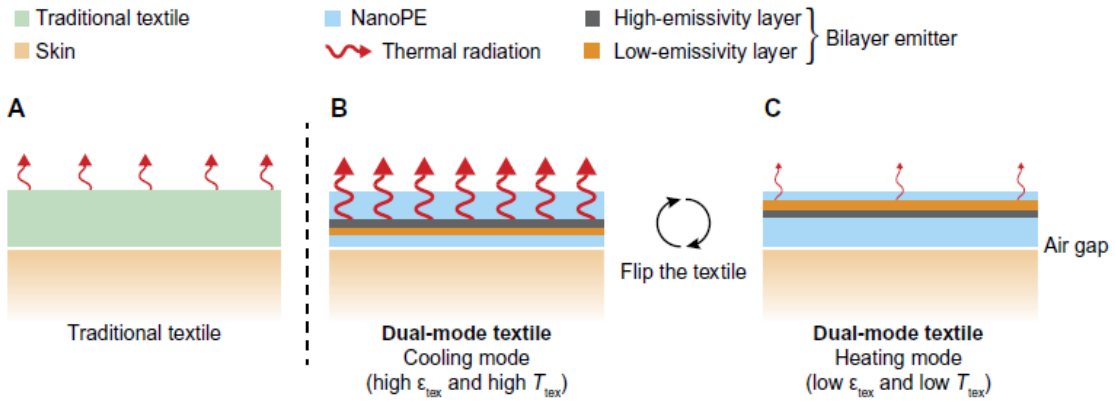

Figure 4. Schematic of dual-mode textile. (A) Traditional textiles only have single emissivity, so the radiation heat transfer coefficient is fixed. (B) For a bilayer thermal emitter embedded in the IR-transparent nanoPE, when the high-emissivity layer faces outside and the nanoPE between the skin and the emitter is thin, the high emissivity and high emitter temperature results in large heat transfer coefficient, so the textile is in cooling mode. (C) The textile is flipped, and the low emissivity and low emitter temperature cause the heat transfer coefficient to decrease. The textile now works in heating mode [37].

A bilayer with asymmetrical emissivity which result in two different heat transfer coefficients is a great advance in passive thermal management with potential application in textiles. However, if textile issues like fashion, comfort and aesthetic are considered, these bilayer materials would not be the best option.

Zhang et al. [43] designed a bimorph fiber of triacetate-cellulose with a thin layer of carbon nanotubes, these fibers were fabricated immersing the bimorph fiber into a CNT solution of various concentrations for 30s, the bimorph fiber was obtained through saponification of triacetate-diacetate fibers converting diacetate in cellulose. This metafibers modulated the infrared radiation of the fabric by more than 35% as the relative

humidity of the wearer skin changed. Each textile yarn is composed of a bundle of metafibers that function via a meta-element (typically a conductive material) added to the polymer textile fibers and a mechanism that responds directly to changes the relative humidity of skin. When humidity is high, the yarn collapses, bringing the metaelements on neighboring fibers closer together to induce resonant electromagnetic coupling. The coupling shifts the emissivity of the textile to better match the human body's thermal radiation, which effectively enhances heat exchange. When humidity is low, the yarn responds in an opposite manner to reduce heat dissipation. The addition of a meta-material adds the possibility of Joule heating in cold weather.

3.4. Polyethylene in thermoregulatory applications

Polyethylene is one of the most common plastics-polyolefins used today. Many unique properties of this material are due its simple molecular structure $(C_2H_4)_n$. Its lightweight, flexibility, and optical transparency in the visible and infrared spectrum makes the polyethylene an excellent alternative to glass [44].

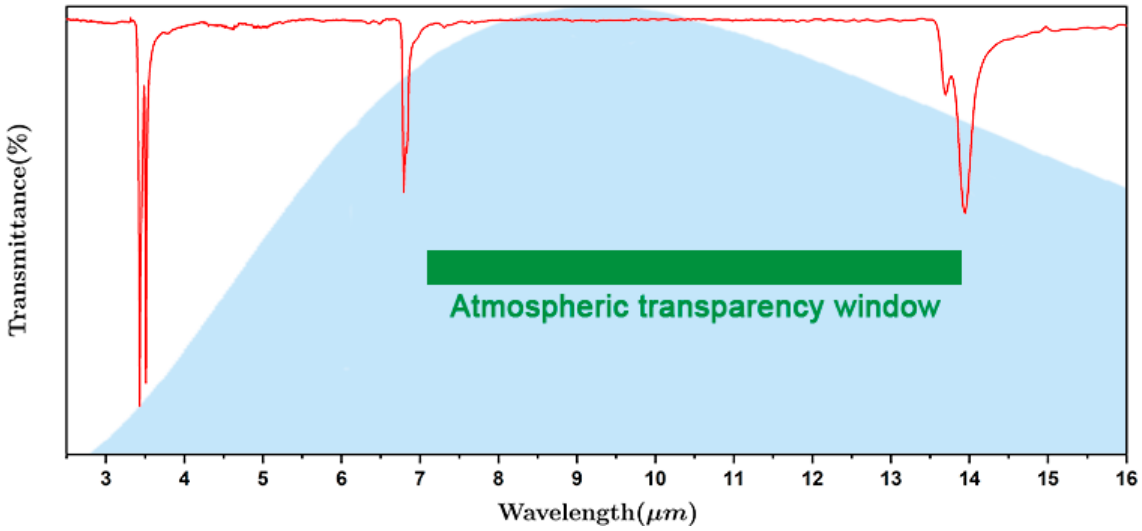

Figure 5. Transmittance of Ultra High Molecular Weight Polyethylene (UHMWPE) film. Mid-infrared transparency window of polyethylene overlaps with the atmospheric transparency window (green range) which coincide with the human body radiation emitted (blue curve), enabling the use of polyethylene in radiative cooling.

The simple structure of this polymer gives a low absorptance in the visible spectrum and in most of the near- and mid-IR spectrum. Many other polymers, like cellulose, silk, polyester, acrylics, absorbs in the mid-to-far IR spectrum, this is due vibrational modes by photoactivation[45], [46]. In the case of polyethylene, the absence of bonds variety limits the number of absorption peaks in the mid-IR, so it is very transparent in the atmospheric transparency window (between 7 and 14 μm wavelength)[47]. The terrestrial objects, also

the human body, emits radiation in the mid-infrared spectrum, with a peak in 9.5 μm, almost all the radiation emitted escape from the Earth surface due the atmospheric transparency window.

3.4.1. Passive radiative cooling of buildings

The radiative cooling of buildings at daytime is challenging, the roofs heat by sunlight absorption. This problem can be treated with surfaces that reflect sunlight efficiently and emit mid-IR radiation [48], [49]. At nighttime, the temperature of buildings roofs goes down below ambient temperature by radiative cooling due low temperatures of outer space of the Earth. This cooling can be improved covering the surfaces with an infrared-transparent material, just like polyethylene, which has been used to prevent the surface heating by air convection[50], [51]. The mid-IR transparency of polyethylene makes it an ideal material to achieve radiative cooling at daytime and nighttime, its optical properties allow to achieve a spectral selectivity embedding nano and micro particles in the polymer matrix[47]. For example, making a polyethylene particle to scatter and reflect sunlight and emit in mid-IR, it must be able to achieve passive radiative cooling at day and night.

3.4.2. Personal passive radiative cooling

Polyethylene can be engineered to reflect and scatter the sunlight keeping efficiently its optical properties in mid-IR. One way to achieve this is to fabricate polyethylene fibers with diameters similar or greater than the solar radiation wavelength, which lead to an ITVOF fabric[10]. Polyethylene fabrics can be opaque in visible range spectrum and remain transparent in mid-IR with fiber diameters similar or larger than solar radiation wavelength but shorter than mid-IR wavelength. Embedding pore in polyethylene fibers can lead to the same effect to scatter visible light and transmit thermal radiation in woven, non-woven and knitted fabrics[9], [52]. These two strategies to control optical properties of polyethylene fabrics let to have potential applications in wearables, bedding, bandages, and apparel[10], [53]–[55]. Other polymer materials with a more complex molecular structure like common polymers in textiles (polyester, cotton, linen, etc.) have multi-band absorption in the infrared spectrum as it can be seen in Figure 3b.

There are some applications of polyethylene in wearables in the market, but they are driven by the material properties (strength, chemical insulation, etc.) and not for its passive thermoregulation. For example, the non-woven micro-fibrous Tyvek HDPE by DuPont are used in laboratory wear[56], also UHMWPE Dyneema fibers by DSM are used in specialty wearables as body armors and helmets, and in abrasion resistant clothing and gloves[57], [58].

3.4.3. Metal-like conductor

Most thermplastic polymers are partially crystalline and partially amorphous with a poor heat conduction (~0.2 $W \cdot m^{-1}K^{-1}$), like water and air thermal conduction, compared with metals (~400 $W \cdot m^{-1}K^{-1}$) and are often used as thermal insulation materials.

Figure 6. Illustration of UHMWPE powder crystallites embedded in a disordered and entangled chain network.

Carbon-based materials have been proven to be potentially the best heat conductors, even better than metals. The fact that polyethylene is composed of a backbone carbon-carbon bonds, like bonds in diamond, makes it a potential conductive material, despite its bulk thermal properties [44], [59]. It has been demonstrated that increasing crystallite orientation and crystallinity increase thermal conductivity in polyethylene, such as isolated and drawn polyethylene nanofibers which provide thermal conductivity higher than some metals (~104 $W \cdot m^{-1}K^{-1}$) [60]. Highly crystalline and stretched polyethylene films and fibers, with oriented polymer chains, provides high thermal conductivity and superior mechanical properties [11], [44], [60]–[65]. Polyethylene materials with high conductivity has been used in conduction of cooling of superconducting magnets and as mitigator of hot spots in solar cells [66], [67]. It has been demonstrated that composite polyethylene-particle films with high thermal conductivity promotes lateral heat spreading away from the locally heated area, making it a potential option to use for passive cooling through radiation [47]. These materials can benefit the wearable technology incorporating thermal conductive polyethylene films and fibers in clothes to deliver heat to the extremities in low temperatures or to remove heat from body areas (like armpit) in high temperatures.

4. MATERIAL AND METHODS

4.1. Materials

The materials used were ultrahigh molecular weight polyethylene in powder form (UHMWPE, molecular weight 3-5x10^6 g/mol, by Sigma-Aldrich) and decalin (Decahydronaphthalene, mixture of cis + trans, anhydrous, ≥99%, by Sigma-Aldrich).

4.2. Polyethylene films

The UHMWPE is dissolved into decalin at 2 w.t.% of polymer concentration and heated at 150°C, which is above the polymer melting temperature (T_m=138°C), for 24 hours in an oil bath. Then, the solution was cast directly onto a glass substrate precooled at -5°C. The films were left inside a fume hood at ambient conditions for three days to let the solvent evaporate. Finally, the cast films were cut in test specimens of 2cmx3cm with a 2cmx1cm drawing zone, as shown in Figure 7. Then, the test specimens were drawn at a rate of 45 mm/min in a universal testing machine (Instron 3365) and heated by convection with a hot air source (T=38°C) to soften the polymer during the drawing process [11], [47], [59]. The stretches were stopped after two checkpoints. The first was when the test specimens were fractured along the stretch axis (tearing) and the second was when it fractured perpendicular to the stretch axis (breaking). Due to stretching limitations of the universal testing machine, after the first checkpoint, a cut in the center of the drawn specimenswas done for obtaining new specimens for further drawing. . The samples in graphs and tables were identified as follows: (1) raw polyethylene as "Powder", (2) casted film without stretching "x0", (3) stretched film 50 times its original size "x50", and (4) stretched film 100 times its original size "x100".

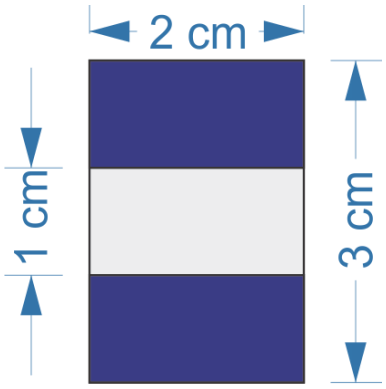

Figure 7. Test tubes for stretching. The blue zone is the part held by the jaws of the universal testing machine, while the white zone is the stretch zone of the film.

4.3. Fourier-Transform Infrared Spectroscopy (FTIR)

To assess the optical properties of polyethylene in the mid-infrared region, infrared spectroscopy was carried out by using a Fourier-Transform Infrared Spectrometer (PerkinElmer, Spectrum 400) equipped with an Attenuated Total Reflectance (ATR) accessory, from 4000 to 400 cm^{-1} with 16 scans for sample and a resolution of 4 cm^{-1}. It is possible to get an estimate of the UHMWPE films' crystallinity with this technique using the bending (1474 and 1464 cm^{-1}) and rocking (730 and 722 cm^{-1}) deformation bands. Zerbi et al [68] suggested an empirical relation:

$$X_{IR\%} = \left(1 - \frac{1-\frac{I_a/I_b}{1.233}}{1+I_a/I_b}\right) * 100 \quad (1)$$

Where $X_{\%}$ is the percentage of crystallinity of the film, I_a is the peak area of polyethylene absorption bands in 1474 and 730 cm^{-1}, I_b is the peak area of polyethylene absorption bands in 1464 and 722 cm^{-1}, and the constant 1.233 corresponds to the relation between these bands for 100% crystalline polyethylene.

4.4. X-Ray Diffraction (XRD)

The fiber alignment after drawning suggests an increase in crystallinity and the arrangement of molecules insides the film. To obtain this information, X-Ray Diffraction (XRD) measurements of the undrawn and drawn films (x50 and x100), were performed using a PanAnalytical (X'Pert Pro PW1800) diffractometer using Cu Kα radiation operated at 45 mA and 40 kV. The data was collected in the 2θ range of 5°-90°. The degree of crystallinity ($X_{XRD\%}$) was calculated using the ratio of the intensities for the crystalline (I_C) and the crystalline + amorphous ($I_C + I_A$) content.

$$X_{XRD\%} = \frac{\sum I_C}{\sum I_C + I_A} * 100 \quad (2)$$

4.5. Differential Scanning Calorimetry (DSC)

After the drawning of the films, the internal fibers align across the drawn axis, which is expected to increase the crystallinity of the film. This effect can be corroborated by Differential Scanning Calorimetry (DSC), which was performed from 20-160°C with a heating rate of 10°C/min in a nitrogen atmosphere. The calculations of the percentage of crystallinity ($X_{DSC\%}$) were performed according to the ASTM F2625 standard. For this, a baseline by connecting points from 50 to 160°C on the first heating run was considered to integrate the endothermic melting peak, which corresponds to the heat of fusion (ΔH_m) of

the sample. Then, the crystallinity ($X_{DSC\%}$) is calculated by dividing such heat of fusion (ΔH_m) by the heat of fusion of 100 % crystalline polyethylene ($\Delta H_m^\circ = 289\, J/g$).

$$X_{DSC\%} = \frac{\Delta H_m}{\Delta H_m^\circ} * 100 \quad (3)$$

4.6. Scanning Electronic Microscopy (SEM)

The SEM images were obtained using a high-resolution scanning electron microscope (SEM, Zeiss, model EVO 25) operated at 10 kV. For SEM imaging, the samples were coated with a 5 nm-thick layer of gold.

4.7. Small and Wide-Angle X-ray Scattering (SWAXS)

The fiber alignment after drawning suggests an increases in crystallinity and the arrangement of molecules insides the film, to obtain this information X-ray scattering in small and wide angle were performed using a Small Angle Scattering system Anton Paar (SAXess mc^2) using Cu Kα radiation. The films were measured in a vacuum chamber to minimize scattering background from air and the damage by radiation. The crystallinity was obtained as in XRD using equation (2). The degree of orientation was estimated using the model proposed by Bandeira et al [69], where they use the Hermans orientation function $\langle P_2 \rangle$:

$$\langle P_2 \rangle = \frac{3\langle \cos^2 \theta \rangle - 1}{2} \quad (4)$$

$$\langle \cos^2 \theta \rangle = \langle \cos^2 \phi_{002,SD} \rangle = 1 - 0.565 \langle \cos^2 \phi_{200,SD} \rangle - 1.4325 \langle \cos^2 \phi_{110,SD} \rangle \quad (5)$$

Where $\phi_{SD} = \frac{\pi}{2} - \phi_{ND}$, being ϕ_{ND} is the angle between the X-Ray reflection plane normal and the plane normal to the draw direction; $\langle \cos^2 \phi_{002,SD} \rangle$ is the degree of orientation of the chain axis ((002) planes), $\langle \cos^2 \phi_{200,SD} \rangle$ and $\langle \cos^2 \phi_{110,SD} \rangle$ are the degree of orientation of the planes (200) and (110) respectively.

5. RESULTS AND DISCUSSION

5.1. Polyethylene films fabrication

The fabrication and drawning of the films were based according to the method reported by Lozano M., et al. [47], but with some modifications. Drawn ratios up to x120 were achieved, dispensing with cooling of substrates with liquid nitrogen and the use of a roll-to-roll system with controlled temperature.

Three films were fabricated (***α, β,*** and ***γ***) under the same conditions, and five test specimens were prepared of each film to carry out the draws in the universal testing machine. The results obtained of each film are presented in Figure 8. The results of draw ratios of each test specimen they mean and standard deviation are presented in Table 1.

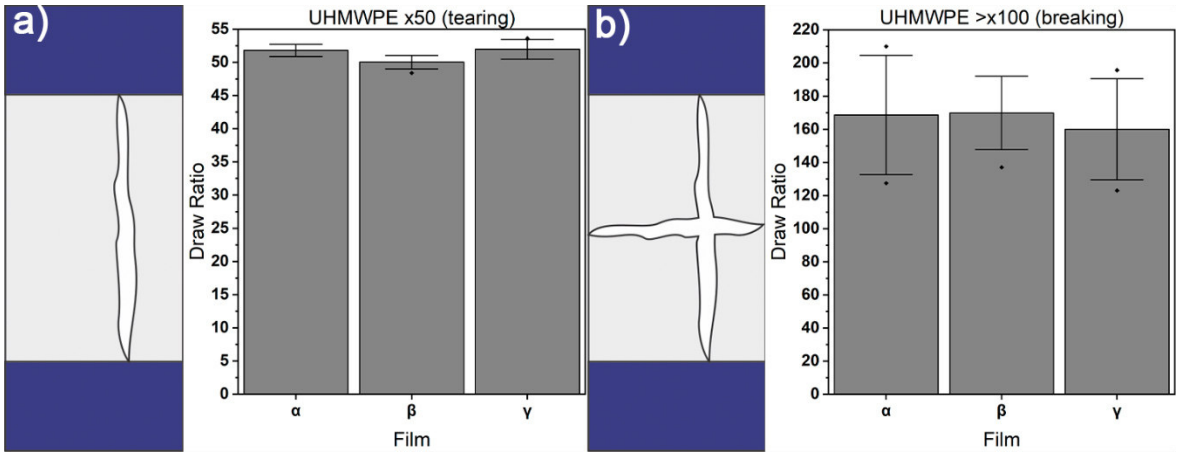

Figure 8. Representation of drawns of each film α, β, and γ, before a fracture a) along to and b) perpendicular to draw axis. The black dot points in film β represents outlier data in that film.

Test specimen	Before fracture along to draw axis			Before fracture perpendicular to draw axis		
	α	***β***	***γ***	***α***	***β***	***γ***
A	51	50	51.1	127.5	185	162
B	52.7	51	50.5	184	178.5	136.3
C	52.5	49.9	53.5	210	184	123
D	51	48.4	53.6	153	179	183
E		50.8	51.1	37	137	195.7
Mean	**51.8**	**50.0**	**52.0**	**168.6**	**172.7**	**160.0**
Std Dev	**0.93**	**1.03**	**1.47**	**35.98**	**20.17**	**30.57**

*Table 1. Results of the five-test specimen of each film (α, β, and γ) before a fracture along to and perpendicular to draw axis, they mean and standard deviation. The missing data in **αE** is due to it fractured perpendicular to the draw axis in the x37 ratio, so this test specimen was not considered for any mean of film **α**.*

Fourteen out of fifteen test specimens were drawn around x50 ratios before a fracture along to the draw axis occured; after that, the process continued achieving ratios above x120 before a fracture perpendicular to the draw axis occured. This method to draw UHMWPE films to ratios of x50 seems to be replicable since means of 51.8±0.93, 50.0±1.03 and 52.0±1.47 were obtained for films α, β, and γ, respectively. In ratios >x100 very close means each other were obtained, but their standard deviations are much higher than ratios around x50.

It was achieved similar draw ratios reported by Lozano M., et al.[47], they reported x60 ratios, and even ratios up to x100 as reported by Loomis J., et al.[11] and Ronca S. et al. [59], using a fixed drawn system compared with the roll-to-roll system, and dispensing the use of liquid nitrogen which reduces costs if this process is carried out to industrial manufacturing.

5.2. Characterization of the films

Four types of samples were measured: UHMWPE powder, UHMWPE x0 (undrawn), UHMWPE x50 and UHMWPE x100 by FTIR (See Appendix A). The spectra were analyzed to determine band absorptions of the films defining the transparency windows of the films in the mid infrared.

In all the measurements, the characteristic absorption bands of UHMWPE were identified (Figure 9). As expected, the characteristic absorption bands of polyethylene remain despite the draw ratio of the films (Figure 10 to 12).

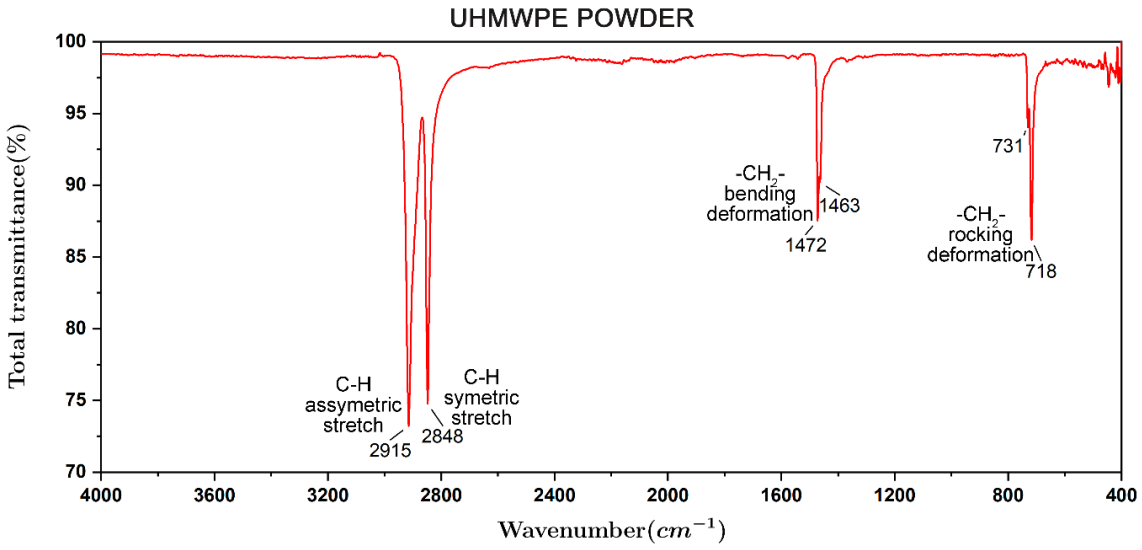

Figure 9. FTIR/ATR spectrum of UHMWPE powder.

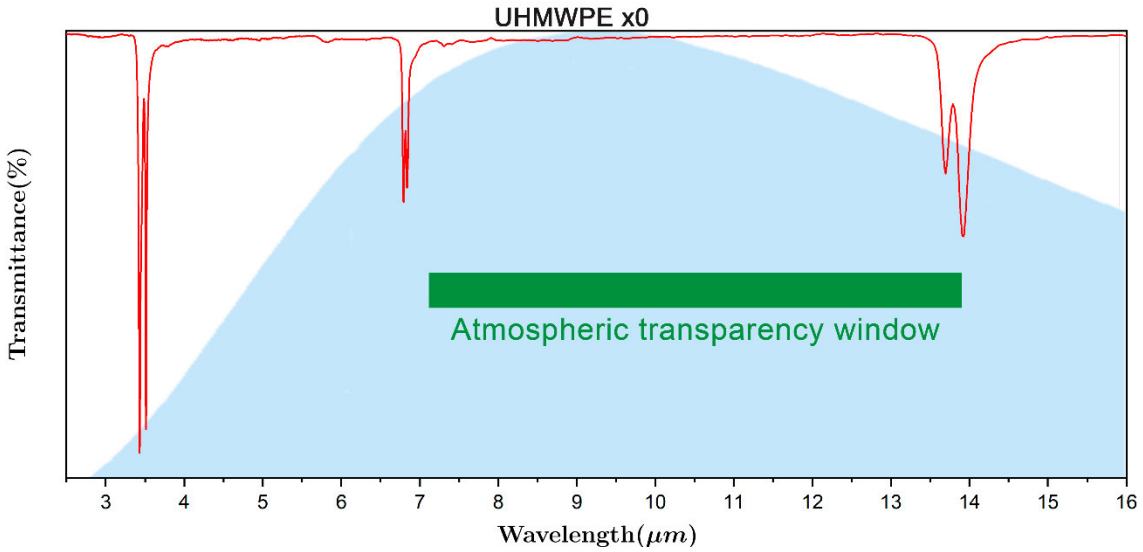

Figure 10. Transparency window of UHMWPE x0 with respect to the human body radiation and the transparency window measured by FTIR/ATR.

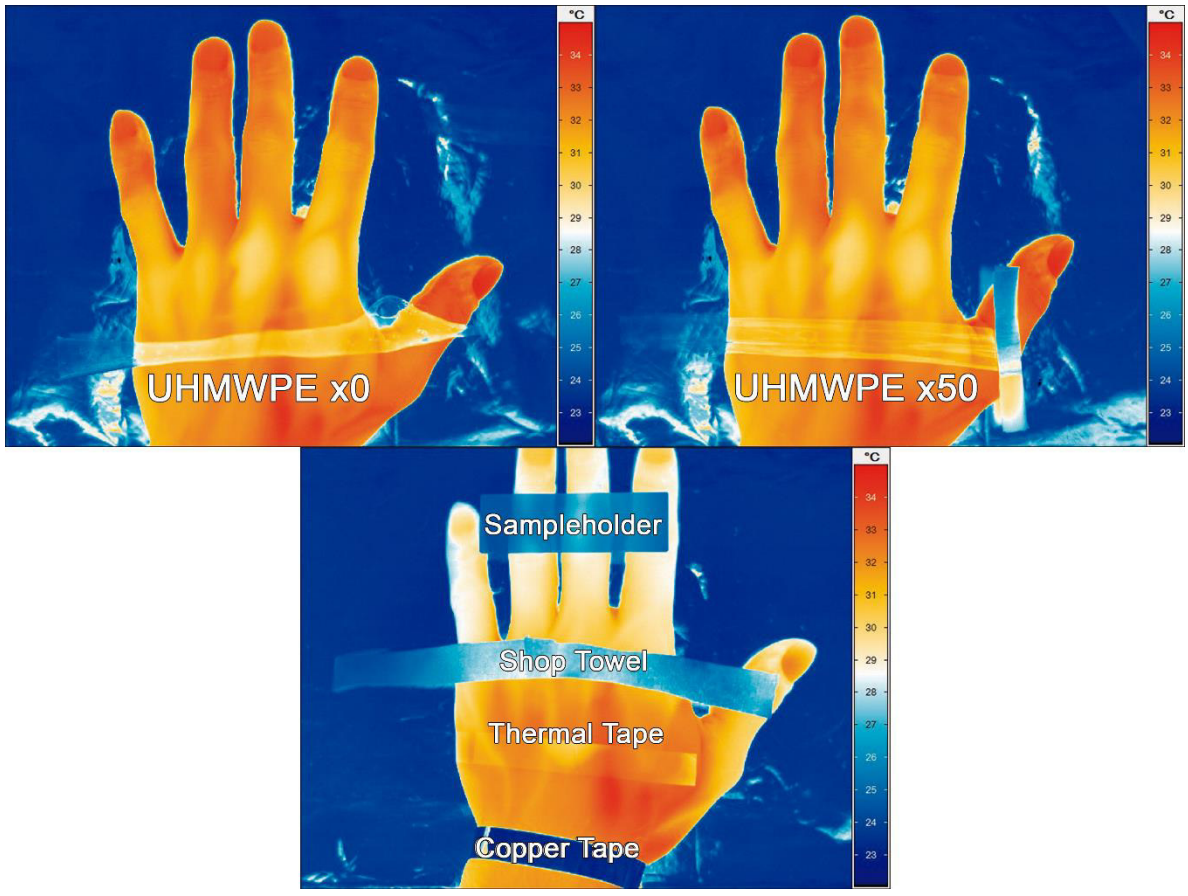

Figure 11. Thermography of UHMWPE x0 and x50 films and other materials to demonstrate the IR transparency of UHMWPE films obtained by IR Camera InfraTec 9500.

To complement the measurement of infrared-transparency of the films' thermography were taken with an IR Camera InfraTec 9500, the thermograms obtained of different materials are shown in Figure 11.

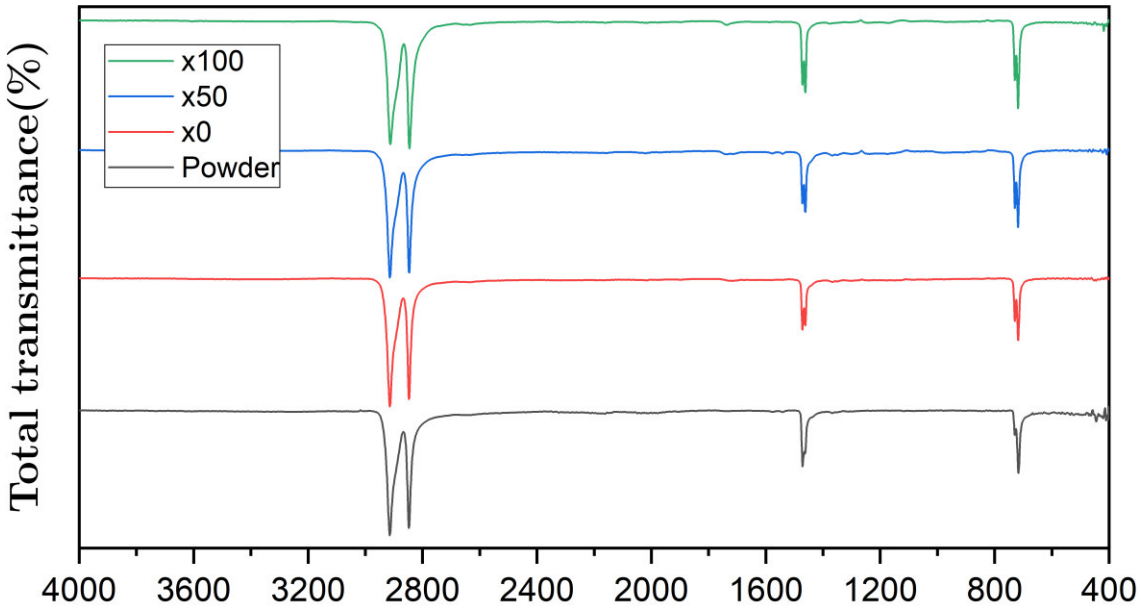

Figure 12. FTIR/ATR spectrum stacking of UHMWPE powder and films x0, x50 and x100.

There must be a re-structuration of the film in the drawing process due mechanical effort and heat applied to the material. To corroborate this assumption some techniques, as XRD, DSC and FTIR, were used to determine a change in the crystallinity film in different draw ratios. Although the main use of FTIR in polymers is not to provide information on crystallinity, some assumptions, and relations to change in crystallinity can be made analyzing the bending (1464 and 1462 cm^{-1}) and rocking (730 and 722 cm^{-1}) deformation absorption bands.

To compare the FTIR spectra of the samples, the data were normalized and plotted (Figure 12, 13 and 14). In Figure 13, it can be observed than in powder sample the absorption band at ≈1462cm^{-1} is not well defined, but in the films (x0, 50 and x100) the two bending absorption bands can be clearly observed. As the draw ratio in films increase, the intensity of the absorption bands also increase, and a change in relative ratio intensity between the two bending bands can be observed in draw films (x50 and x100).

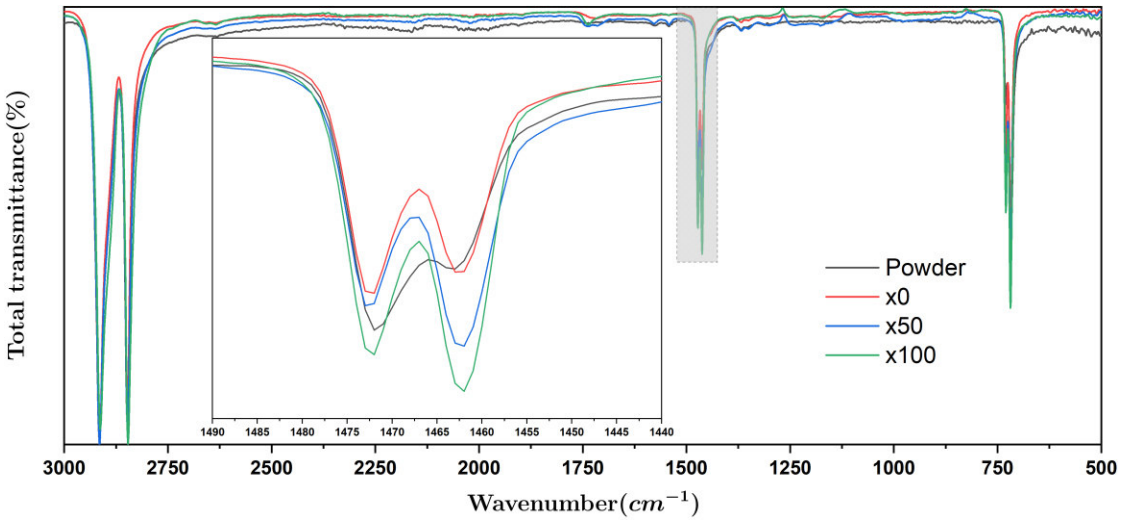

Figure 13. Comparison on bending deformation absorption bands in UHMWPE Powder, and x0, x50 and x100 films.

In Figure 14, the comparison between the rocking bands (730 and 722 cm^{-1}) were plotted. As in Figure 13, the absorption band in ≈730 cm^{-1} is not as well-defined in the powder sample as it is in the films. There is also an increase in intensity according to an increase in the draw ratio. These increases in intensity in the absorption bands can be related to a change in crystallinity/structure of the film.

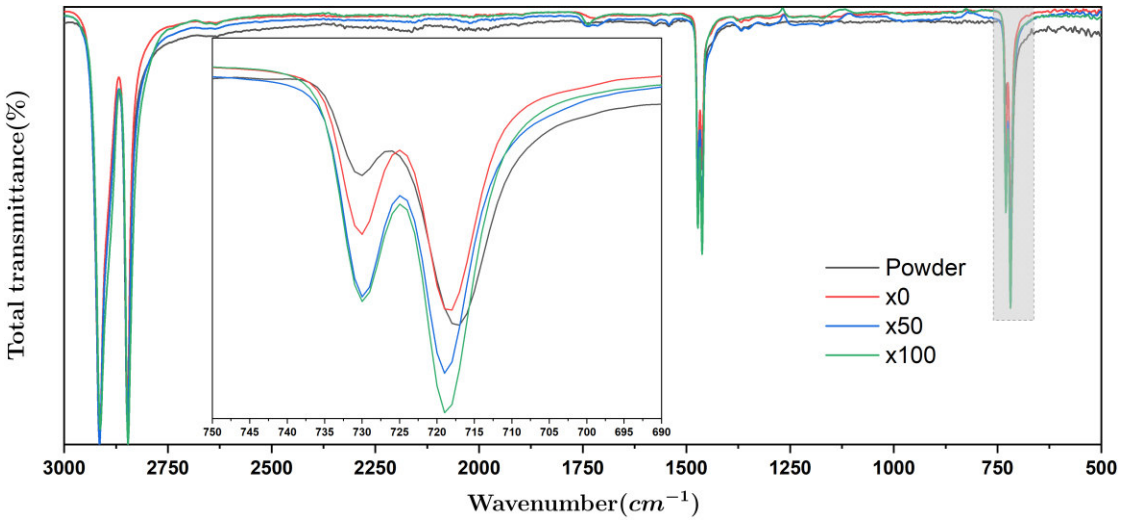

Figure 14. Comparison on rocking deformation absorption bands in UHMWPE Powder, and x0, x50 and x100 films.

To obtain an approximation on crystallization changes according to draw ratios, band fitting techniques were used to obtain the peaks areas to apply (1). The results are summarized in Table 3. The accuracy of this method is not high but gives a very acceptable estimate of the crystallinity of the films and give an idea how it changes as the draw ratio increases. According to the results reported by Hamzah et al. [70] and Pagés [70], the

absorption bands at 1464/1462 cm^{-1} give a better approximation to crystallinity information of polyethylene films than the bands at 730/722 cm^{-1}.

Sample	Area		$\frac{I_a}{I_b}$	$X_{IR\%}$	Area		$\frac{I_a}{I_b}$	$X_{IR\%}$
	I730	I722			I1464	I1462		
Powder	0.12	0.65	0.19	**29**	0.24	0.51	0.46	**63**
X0	0.56	1.17	0.47	**58**	0.67	0.75	0.90	**86**
x50	0.84	1.61	0.52	**62**	0.74	1.10	0.67	**73**
x100	0.94	1.87	0.50	**61**	1.06	1.28	0.83	**82**

Table 2. Variation of crystallinity in UHMWPE Films with different draw ratios by FTIR.

The XRD patterns obtained show peaks at around 21.5° and 23.9°, which are associated respectively to the diffraction planes (110) and (200) of the orthorhombic unit cell of UHMWPE. It can be observed in Figure 15 how the amorphous band of the x0 film disappear in the x50 and x100 films, which indicate a higher crystallinity in the samples. There is an increment in the relative ratio in the intensity between the peaks corresponding to the planes (110) and (200) in the x50 and x100 films, which indicate a preferred ordering to the plane (110) along the drawing process. The other peaks around 40° and 50° in the film x0 indicates other diffraction planes of the material (36.6° to (020), 41.6° to (111), and 42.9° to (201)).

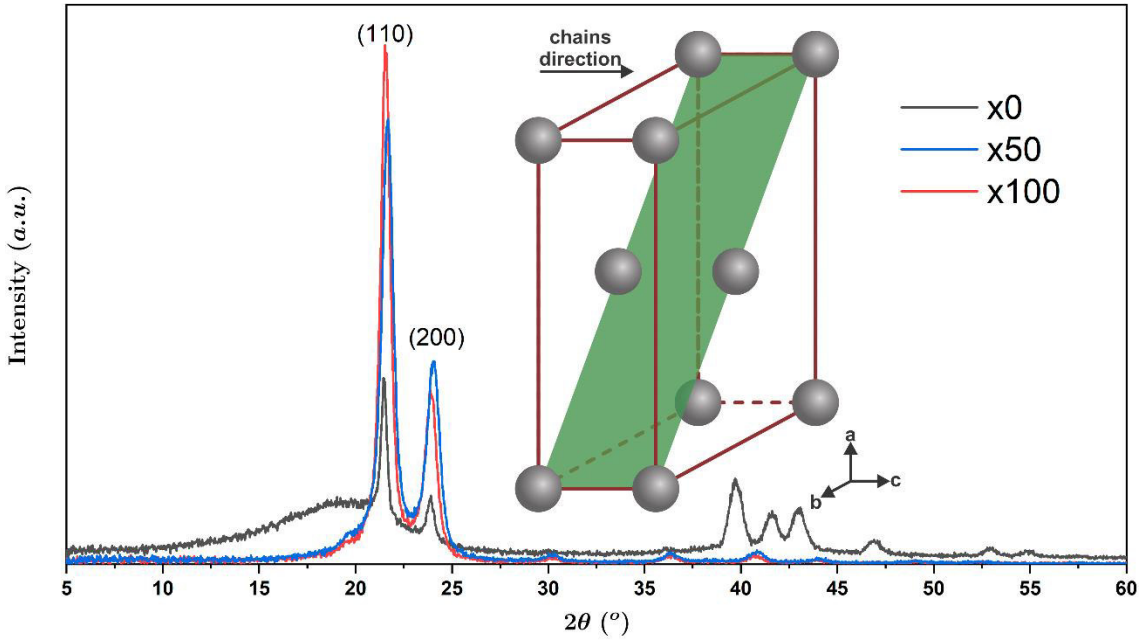

Figure 15. X-Ray diffractogram of UHMWPE film x0, x50 and x100.

Using equation (2), an approximation of the degree of crystallinity ($X_{XRD\%}$) can be obtained (Table 3).

Sample	Area		X_{XRD}%
	Crystalline peaks	Crystalline + Amorphous	
Powder	19910.04	44722.66	**38**
x0	4892.09	8569.25	**28**
x50	7010.41	7515.91	**93**
x100	6554.67	6811.70	**96**

Table 3. Degree of crystallinity calculated from x-ray diffractogram.

The first heating of the thermograms from DSC obtained for different samples (powder, film x0, 50, and x100) is shown in Figure 16. The melting temperature (T_m) shifting of the UHMWPE x0 film with respect to UHMWPE Powder (from 142.8°C to 138.1°C) indicates that there is a restructuring when the UHMWPE powder is dissolved in decalin and heated for 24 hours, the lower melting temperature of this film means that it needs less energy to a phase change than the UHMWPE powder.

Then when the film is drawn, it restructures to a more ordered material, which is indicated by the T_m, peak shift from 138.1 °C to 142.3-143.8 °C, now the material needs more energy to melt. The peak thinning of the x50 and x100 films thermograms, with respect to thex0 film and UHMWPE powder, indicates a smaller distribution of crystalline grain sizes within the material.

Using equation (3), an approximation of the degree of crystallinity ($X_{DSC\%}$) can be obtained from DSC. The results, melting temperature (T_m) and the onset temperature (T_{onset}) of the samples are shown in table 4.

Sample	T_{onset} [°C]	T_m [°C]	ΔH $\left[\frac{J}{g}\right]$	X_{DSC}%
Powder	133.53	142.8	148.32	**51**
x0	130.67	138.1	203.85	**70**
x50	138.77	142.3	165.98	**57**
x100	140.09	143.8	187.28	**65**

Table 4. Degree of crystallinity calculated from DSC.

The increase in crystallinity in the x0 film with respect to powder indicates that there is a restructuring of the material, but this increase in crystallinity is accompanied by a wide distribution of crystal sizes in the material. On the other hand, in the drawn films there is less crystallinity than the x0 film, this could be due a forced restructuring by mechanical tension assisted with heat which align the crystals to a preferred direction according to the XRD results as the draw ratio increase, this assumption is confirmed with the increase of the onset temperature (T_{onset}) from UHMWPE x0 and UHMWPE x50 and x100. As shown in Table 4, when the half of the crystals in UHMPE x0 sample are melted (at the T_m point) the

UHMWPE x50 Sample crystals just begin to melt (T_{onset}). So, there could be less crystallinity in the drawn films than the casted films, but there is a smaller crystalline grain size distribution and a preferred alignment.

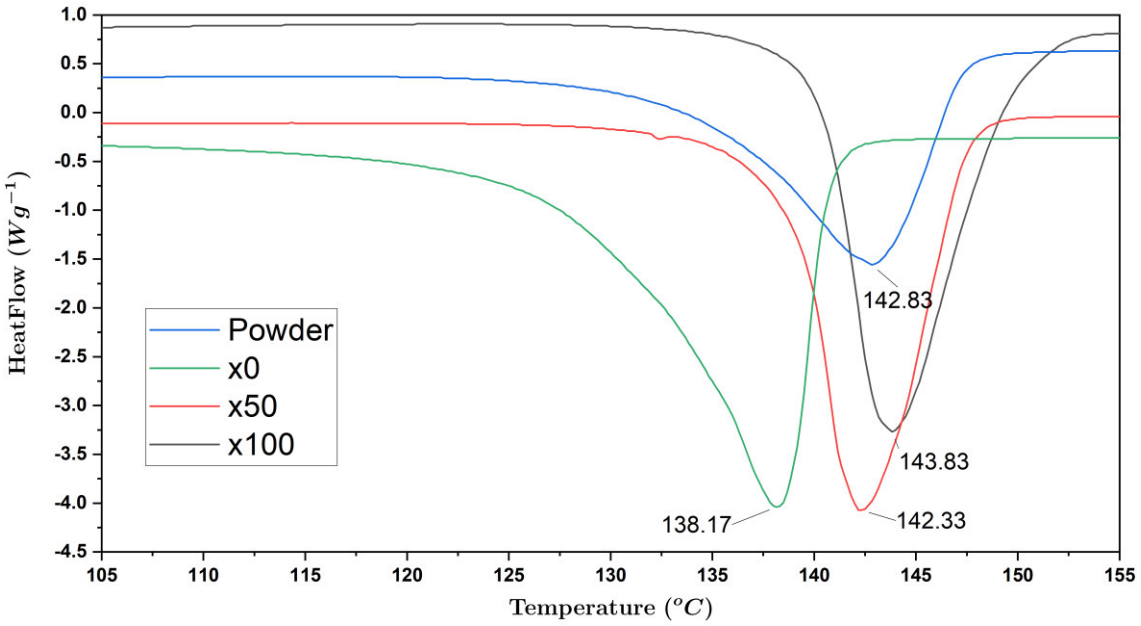

Figure 16. First heat thermogram's DSC of UHMWPE powder sample and film x0, x50 and x100 samples.

In Table 5, the results of the crystallinity measurements obtained from three different techniques are shown (only the analysis of the absorption bands at 1464/1462 cm^{-1} in FTIR is shown).

Sample	$X_{XRD\%}$	$X_{DSC\%}$
Powder	38	51
x0	28	70
x50	93	57
x100	96	65

Table 5. Results of crystallinity from FTIR-ATR, XRD and DSC.

The crystallinity obtained by FTIR and DSC shows a similar behavior, which confirms the objective of the crystallinity estimation from FTIR proposed by Zerbi, et al. [68], [72].

The increase in the alignment of the internal fibers composing the films was demonstrated with SEM images and 2D diffractograms patterns by WAXS (Figure 17). The film surface of UHMWPE film x0 shows how the UHMWPE powder after the dissolution and casting process is disordered and results in a rough surface. As the draw ratio increases (Figure 17b-c), the orientation of film fibers is more evident, and fibers diameters is reduced giving a smoother texture of the film. Some roughness measurements were carried on in an optical 3D surface measurement system Bruker Alicona model Infinite Focus. The result of

the x50 film was a value of Ra of 343 nm perpendicular to the drawn axis and for the x100 film the result was 170 nm.

The 2D patterns obtained by WAXS demonstrate the change from an isotropic (Figure 17d) to an anisotropic material (Figure 17e) to an increment in the draw ratio, the prefer alignment to the draw axis is observable in the UHMWPE film x100 (Figure 16e) and the degree of orientation is calculated using equation (4) and (5), the results are shown in Table 6. The most intense peak diffraction is the plane (110) as was obtained by XRD (Figure 14).

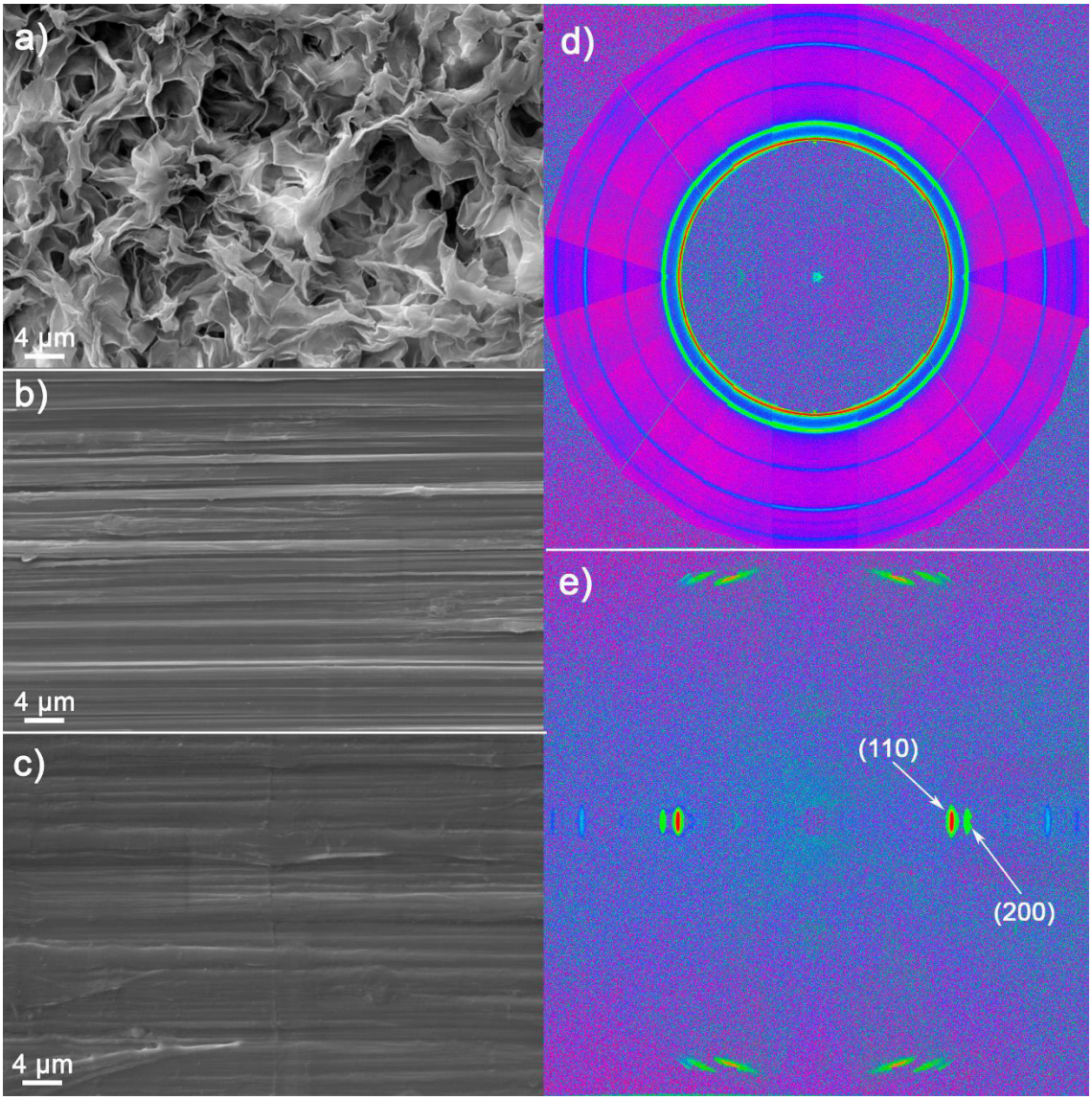

Figure 17. SEM images of UHMWPE films a) x0, b) x50 and c) x100 and WAXS 2D diffractograms patterns obtained from UHMWPE films d) x0 and e) x100, which demonstrate the alignment of the fibers (SEM) and crystallites (WAXS) along the draw axis.

Sample	$\langle \cos^2 \theta \rangle$	$\langle P_2 \rangle$
x0	-	0
x100	0.99	0.98

Table 6. Results of orientation estimated by WAXS 2D patterns.

As expected, a change in crystallinity and an increase in the order (alignment of crystalline grains and fibers) of the material while the draw ratio increases, as it is reported in the literature [38], [55], [59], [60], [68], [70]–[72]. A scheme of the restructuration and orientation of the films are shown in Figure 17.

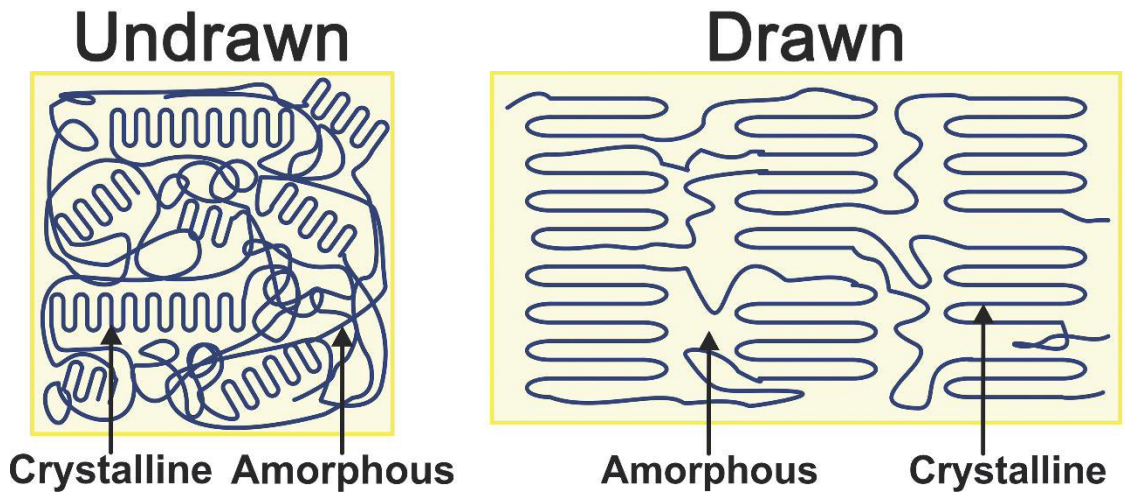

Figure 18. Schematic representation of an undrawn films and the restructuration of the film after the draw process. The alignment of the crystals and fibers along the stretch axis increase.

6. FUTURE WORK

In the near future, there is the proposal to characterize the UHMWPE films to qualitatively compare their thermal conductivity. The proposal is based on the model proposed by [73] as follows: Using an infrared camera ImageIR 9500 from InfraTec it can be analyzed how the films transport heat. The heat is going to be induced by visible light of a projector. The sample will be placed into a vacuum chamber, to reduce the heat loss by convection and air-surface conduction, this chamber will have two optical windows, a visible window with high/low transmissivity in the visible/infrared range (made of silica, for example) and an infrared window (could be made of Ge, ZnSe, etc.). The visible window will have a rectangular collimator to analyze a section of the film and the difference of temperature on the film, to calculate and get a precise estimation of thermal conductivity a thermal resistor will be placed into the vacuum chamber and connected to a multimeter.

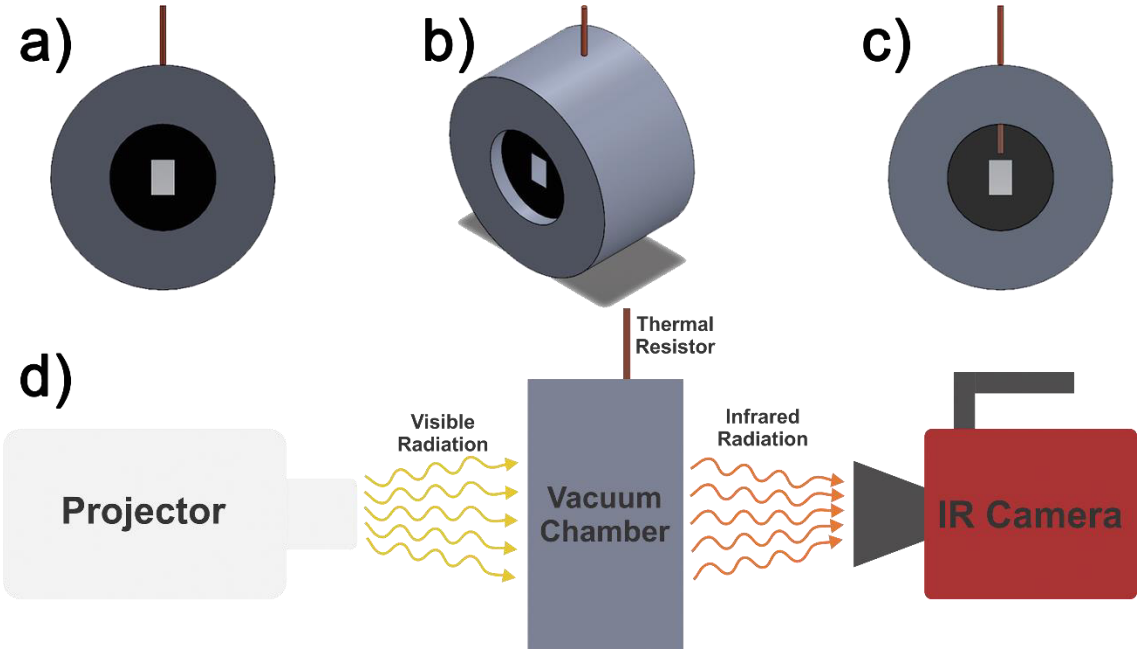

Figure 19. Prototype of thermal conductivity characterization. a) Is the back view of vacuum chamber (visible window with the collimator), b) is an isometric view of the vacuum chamber it can be appreciated the thermal resistor at the top of the chamber, c) is the front view of the vacuum chamber (infrared window). d) Schematic representation of the design of the thermal measurement arrangement.

There are some improvement areas in this project, for example, the drawing of the films with a controlled heat source. There is a universal testing machine with an oven coupled which would let to control the temperature of the environment, which could help to get higher draw ratios. Besides, the use of a plasticizer (just as LDPE) would increase the draw ratios reached in the films.

Another improvement area would be the use of a Coette-flow extruder to homogenize the casted films and their thickness.

More characterization techniques and analysis could be made to create a complete structure image of the changes in the films as they are drawn.

7. CONCLUSIONS

Ultra-oriented UHMWPE films were obtained with draw ratios above of x100 using an alternative method than the reported in the literature, using the cast method but cooling the substrates in a cooler instead of using liquid-nitrogen and applying a uniaxial drawn method with lower temperature (T=38°C) than reported (T=90 to 120°C).

After the applied engineering to UHMWPE films was done, the mid-infrared properties (transmittance) were preserved, which allows the material to has potential applications in passive cooling for personal thermal management. The structure order (crystallinity, and alignment of chains and fibers) was modified, DSC measurements give an idea of the crystal's quantity in the sample, regardless of its size, distribution, and orientation. While XRD crystallinity provides information about crystal lattice, the size of the unit cell and crystals orientation along the film, this last one is closely related to the fiber orientation and alignment along the film as it is demonstrated in SEM images and WAXS patterns. The crystallinity analysis, orientation results from WAXS and SEM images provide a complete picture of the material structure from the nanoscale to the microscale. As reported in the literature, the thermal conductivity depends in a certain way on the crystallinity and alignment of UHMWPE films, higher crystallinity along with greater ordering and alignment of the chains and fibers in the film suggests an increase in thermal conductivity. This property provides the materials a window to be applied not only in personal thermal management devices but also in electronic or any device used in applications where heat is involved.

More measurements are needed to obtain quantitative data of properties such as thermal conductivity and mid-IR transmission, absorption, and reflection quantitatively.

8. REFERENCES

[1] L. Schellen, M. G. L. C. Loomans, B. R. M. Kingma, M. H. de Wit, A. J. H. Frijns, and W. D. van Marken Lichtenbelt, "The use of a thermophysiological model in the built environment to predict thermal sensation: Coupling with the indoor environment and thermal sensation," *Building and Environment*, vol. 59, pp. 10–22, 2013, doi: 10.1016/j.buildenv.2012.07.010.

[2] L. Schellen, M. G. L. C. Loomans, M. H. de Wit, B. W. Olesen, and W. D. van M. Lichtenbelt, "The influence of local effects on thermal sensation under non-uniform environmental conditions - Gender differences in thermophysiology, thermal comfort and productivity during convective and radiant cooling," *Physiology and Behavior*, vol. 107, no. 2, pp. 252–261, 2012, doi: 10.1016/j.physbeh.2012.07.008.

[3] J. L. M. Hensen, "Literature review on thermal comfort in transient conditions," *Building and Environment*, vol. 25, no. 4, pp. 309–316, 1990, doi: 10.1016/0360-1323(90)90004-B.

[4] A. P. Gagge, J. A. J. Stolwijk, and J. D. Hardy, "Comfort and thermal sensations and associated physiological responses at various ambient temperatures," *Environmental Research*, vol. 1, no. 1, pp. 1–20, 1967, doi: 10.1016/0013-9351(67)90002-3.

[5] S. Seyam, "Types of HVAC Systems," *HVAC System*, 2018, doi: 10.5772/intechopen.78942.

[6] T. Hoyt, K. H. Lee, H. Zhang, E. Arens, and T. Webster, "Indoor Environmental Quality (IEQ) Title Energy savings from extended air temperature setpoints and reductions in room air mixing Publication Date ENERGY SAVINGS FROM EXTENDED AIR TEMPERATURE SETPOINTS AND REDUCTIONS IN ROOM AIR MIXING," *International Conference on Environmental Ergonomics*, 2009.

[7] L. Pérez-Lombard, J. Ortiz, and C. Pout, "A review on buildings energy consumption information," *Energy and Buildings*, vol. 40, no. 3, pp. 394–398, 2008, doi: 10.1016/j.enbuild.2007.03.007.

[8] M. Jain, R. K. Kalaimani, S. Keshav, and C. Rosenberg, "Using personal environmental comfort systems to mitigate the impact of occupancy prediction errors on HVAC performance," *Energy Informatics*, vol. 1, no. 1, pp. 1–21, 2018, doi: 10.1186/s42162-018-0064-9.

[9] P. C. Hsu *et al.*, "Radiative human body cooling by nanoporous polyethylene textile," *Science*, vol. 353, no. 6303, pp. 1019–1023, 2016, doi: 10.1126/science.aaf5471.

[10] J. K. Tong, X. Huang, S. V. Boriskina, J. Loomis, Y. Xu, and G. Chen, "Infrared-Transparent Visible-Opaque Fabrics for Wearable Personal Thermal Management," *ACS Photonics*, vol. 2, no. 6, pp. 769–778, 2015, doi: 10.1021/acsphotonics.5b00140.

[11] J. Loomis *et al.*, "Continuous fabrication platform for highly aligned polymer films," *TECHNOLOGY*, vol. 02, no. 03, pp. 189–199, Sep. 2014, doi: 10.1142/S2339547814500216.

[12] L. Wang, H. Yin, Y. Di, Y. Liu, and J. Liu, "Human local and total heat losses in different temperature," *Physiology and Behavior*, vol. 157, pp. 270–276, 2016, doi: 10.1016/j.physbeh.2016.02.018.

[13] K. C. Mendoza and J. D. Griffin, “Thermoregulation,” G. F. Koob, M. Le Moal, and R. F. B. T.-E. of B. N. Thompson, Eds. Oxford: Academic Press, 2010, pp. 400–404. doi: https://doi.org/10.1016/B978-0-08-045396-5.00169-X.

[14] W. Song, F. Wang, and F. Wei, “Hybrid cooling clothing to improve thermal comfort of office workers in a hot indoor environment,” *Building and Environment*, vol. 100, pp. 92–101, 2016, doi: 10.1016/j.buildenv.2016.02.009.

[15] M. Zhao, C. Gao, J. Li, and F. Wang, “Effects of two cooling garments on post-exercise thermal comfort of female subjects in the heat,” *Fibers and Polymers*, vol. 16, no. 6, pp. 1403–1409, 2015, doi: 10.1007/s12221-015-1403-0.

[16] C. Zhang, C. Ren, Y. Li, W. Song, P. Xu, and F. Wang, “Designing a smart electrically heated sleeping bag to improve wearers’ feet thermal comfort while sleeping in a cold ambient environment,” *Textile Research Journal*, vol. 87, no. 10, pp. 1251–1260, 2017, doi: 10.1177/0040517516651104.

[17] T. Zhang *et al.*, “High-performance, flexible, and ultralong crystalline thermoelectric fibers,” *Nano Energy*, vol. 41, pp. 35–42, 2017, doi: 10.1016/j.nanoen.2017.09.019.

[18] Z. Li, Z. Xu, Y. Liu, R. Wang, and C. Gao, “Multifunctional non-woven fabrics of interfused graphene fibres,” *Nature Communications*, vol. 7, pp. 1–11, 2016, doi: 10.1038/ncomms13684.

[19] Y. Q. Li *et al.*, “Multifunctional Wearable Device Based on Flexible and Conductive Carbon Sponge/Polydimethylsiloxane Composite,” *ACS Applied Materials and Interfaces*, vol. 8, no. 48, pp. 33189–33196, 2016, doi: 10.1021/acsami.6b11196.

[20] H. Qi, J. Liu, and E. Mäder, “Smart cellulose fibers coated with carbon nanotube networks,” *Fibers*, vol. 2, no. 4, pp. 295–307, 2014, doi: 10.3390/fib2040295.

[21] E. Khalil, “Application of Phase Change Materials in in Textiles: A Review,” *Advanced Materials Research*, vol. 2, no. May, pp. 281–294, 2015, doi: 10.4028/www.scientific.net/amr.1096.533.

[22] G. Bartkowiak, A. Dabrowska, and A. Marszalek, “Assessment of an active liquid cooling garment intended for use in a hot environment,” *Applied Ergonomics*, vol. 58, pp. 182–189, 2017, doi: 10.1016/j.apergo.2016.06.009.

[23] G. Erkan, “Enhancing The Thermal Properties of Textiles With Phase Change Materials,” *Research Journal of Textile and Apparel*, vol. 8, no. 2, pp. 57–64, 2004, doi: 10.1108/RJTA-08-02-2004-B008.

[24] M. Itani, N. Ghaddar, D. Ouahrani, K. Ghali, and B. Khater, “An optimal two-bout strategy with phase change material cooling vests to improve comfort in hot environment,” *Journal of Thermal Biology*, vol. 72, no. December 2017, pp. 10–25, 2018, doi: 10.1016/j.jtherbio.2017.12.005.

[25] D. Benmoussa, K. Molnar, H. Hannache, and O. Cherkaoui, “Novel Thermo-Regulating Comfort Textile Based on Poly(allyl ethylene diamine)/n-Hexadecane Microcapsules Grafted

onto Cotton Fabric," *Advances in Polymer Technology*, vol. 37, no. 2, pp. 419–428, 2018, doi: 10.1002/adv.21682.

[26] O. Troynikov and W. Wardiningsih, "Moisture management properties of wool/ polyester and wool/bamboo knitted fabrics for the sportswear base layer," *Textile Research Journal*, vol. 81, no. 6, pp. 621–631, 2011, doi: 10.1177/0040517510392461.

[27] M. Senthilkumar, M. B. Sampath, and T. Ramachandran, "Moisture Management in an Active Sportswear: Techniques and Evaluation—A Review Article," *Journal of The Institution of Engineers (India): Series E*, vol. 93, no. 2, pp. 61–68, 2012, doi: 10.1007/s40034-013-0013-x.

[28] S. Mukhopadhyay, "Microfibres - An overview," *Indian Journal of Fibre and Textile Research*, vol. 27, no. 3, pp. 307–314, 2002.

[29] J. Venkatesh and K. N. N. Gowda, "Effect of Plasma Treatment on the Moisture Management Properties of Regenerated Bamboo Fabric," vol. 3, no. 10, pp. 1–8, 2013.

[30] V. Thangavelu and P. Chidambaram, "Comparison of moisture management properties of plasma treated single Jersey fabric with different types of polyester yarns," *Fibres and Textiles in Eastern Europe*, vol. 27, no. 1, pp. 32–36, 2019, doi: 10.5604/01.3001.0012.7505.

[31] M. Manshahia and A. Das, "High active sportswear – a critical review," *Indian Journal of Fibre and Textile Research*, vol. 39, no. 4, pp. 441–449, 2014.

[32] Y. Dong, J. Kong, S. L. Phua, C. Zhao, N. L. Thomas, and X. Lu, "Tailoring surface hydrophilicity of porous electrospun nanofibers to enhance capillary and push-pull effects for moisture wicking," *ACS Applied Materials and Interfaces*, vol. 6, no. 16, pp. 14087–14095, 2014, doi: 10.1021/am503417w.

[33] P. Yang, C. Chen, and Z. M. Zhang, "A dual-layer structure with record-high solar reflectance for daytime radiative cooling," *Solar Energy*, vol. 169, no. December 2017, pp. 316–324, 2018, doi: 10.1016/j.solener.2018.04.031.

[34] Y. Cui, H. Gong, Y. Wang, D. Li, and H. Bai, "A Thermally Insulating Textile Inspired by Polar Bear Hair," *Advanced Materials*, vol. 30, no. 14, pp. 1–8, 2018, doi: 10.1002/adma.201706807.

[35] N. N. Shi, C. C. Tsai, F. Camino, G. D. Bernard, N. Yu, and R. Wehner, "Keeping cool: Enhanced optical reflection and radiative heat dissipation in Saharan silver ants," *Science*, vol. 349, no. 6245, pp. 298–301, 2015, doi: 10.1126/science.aab3564.

[36] Y. N. Song, Y. Li, D. X. Yan, J. Lei, and Z. M. Li, "Novel passive cooling composite textile for both outdoor and indoor personal thermal management," *Composites Part A: Applied Science and Manufacturing*, vol. 130, no. 24, p. 105738, 2020, doi: 10.1016/j.compositesa.2019.105738.

[37] P. Hsu *et al.*, "A dual-mode textile for human body radiative heating and Cooling," no. November, pp. 1–8, 2017.

[38] P. C. Hsu *et al.*, “Personal thermal management by metallic nanowire-coated textile,” *Nano Letters*, vol. 15, no. 1, pp. 365–371, 2015, doi: 10.1021/nl5036572.

[39] L. Cai *et al.*, “Warming up human body by nanoporous metallized polyethylene textile,” *Nature Communications*, vol. 8, no. 1, 2017, doi: 10.1038/s41467-017-00614-4.

[40] J. F. V. Vincent, O. A. Bogatyreva, N. R. Bogatyrev, A. Bowyer, and A.-K. Pahl, “Biomimetics: its practice and theory,” *Journal of The Royal Society Interface*, vol. 3, no. 9, pp. 471–482, Aug. 2006, doi: 10.1098/rsif.2006.0127.

[41] E. M. Leung *et al.*, “A dynamic thermoregulatory material inspired by squid skin,” *Nature Communications*, vol. 10, no. 1, pp. 1–10, 2019, doi: 10.1038/s41467-019-09589-w.

[42] X. Yue, T. Zhang, D. Yang, F. Qiu, G. Wei, and H. Zhou, “Multifunctional Janus fibrous hybrid membranes with sandwich structure for on-demand personal thermal management,” *Nano Energy*, vol. 63, no. June, p. 103808, 2019, doi: 10.1016/j.nanoen.2019.06.004.

[43] X. A. Zhang *et al.*, “Dynamic gating of infrared radiation in a textile,” *Science*, vol. 363, no. 6427, pp. 619–623, 2019, doi: 10.1126/science.aau1217.

[44] S. V. Boriskina, “An ode to polyethylene,” *MRS Energy & Sustainability*, vol. 6, no. 1, p. 14, Jun. 2019, doi: 10.1557/mre.2019.15.

[45] T. Okada and L. Mandelkern, “Effect of morphology and degree of crystallinity on the infrared absorption spectra of linear polyethylene,” *Journal of Polymer Science Part A-2: Polymer Physics*, vol. 5, no. 2, pp. 239–262, 1967, doi: 10.1002/pol.1967.160050201.

[46] S. Krimm, C. Y. Liang, and G. B. B. M. Sutherland, “Infrared spectra of high polymers. II. Polyethylene,” *The Journal of Chemical Physics*, vol. 25, no. 3, pp. 549–562, 1956, doi: 10.1063/1.1742963.

[47] L. M. Lozano *et al.*, “Optical engineering of polymer materials and composites for simultaneous color and thermal management,” *Optical Materials Express*, vol. 9, no. 5, p. 1990, 2019, doi: 10.1364/ome.9.001990.

[48] S. V. Boriskina *et al.*, “Roadmap on optical energy conversion,” *Journal of Optics (United Kingdom)*, vol. 18, no. 7, 2016, doi: 10.1088/2040-8978/18/7/073004.

[49] C. G. Granqvist, A. Hjortsberg, and T. S. Eriksson, “Radiative cooling to low temperatures with selectivity IR-emitting surfaces,” *Thin Solid Films*, vol. 90, no. 2, pp. 187–190, 1982, doi: 10.1016/0040-6090(82)90648-4.

[50] M. Santamouris and J. Feng, “Recent progress in daytime radiative cooling: Is it the air conditioner of the future?,” *Buildings*, vol. 8, no. 12, 2018, doi: 10.3390/buildings8120168.

[51] G. Smith, A. Gentle, M. Arnold, and M. Cortie, “Nanophotonics-enabled smart windows, buildings and wearables,” *Nanophotonics*, vol. 5, no. 1, pp. 55–73, 2016, doi: 10.1515/nanoph-2016-0014.

[52] B. Bhatia *et al.*, “Passive directional sub-ambient daytime radiative cooling,” *Nature Communications*, vol. 9, no. 1, pp. 1–8, 2018, doi: 10.1038/s41467-018-07293-9.

[53] S. V. Boriskina *et al.*, "Heat meets light on the nanoscale," *Nanophotonics*, vol. 5, no. 1, pp. 134–160, 2016, doi: 10.1515/nanoph-2016-0010.

[54] Y. Peng *et al.*, "Nanoporous polyethylene microfibres for large-scale radiative cooling fabric," *Nature Sustainability*, vol. 1, no. 2, pp. 105–112, 2018, doi: 10.1038/s41893-018-0023-2.

[55] A. Yang *et al.*, "Thermal Management in Nanofiber-Based Face Mask," *Nano Letters*, vol. 17, no. 6, pp. 3506–3510, 2017, doi: 10.1021/acs.nanolett.7b00579.

[56] USA DuPont, "Tyvek." http://www.dupont.com/products-andservices/%0Afabrics-fibers-nonwovens/protective-fabrics/brands/tyvek.html

[57] J. A. P. M. Simmelink, J. J. Mencke, M. J. N. Jacobs, and R. Marissen, "Process for making high-performance polyethylene multifilament yarn," Patent No: US9759525B2

[58] Y. Fukushima, H. Murase, and Y. Ohta, "Dyneema®: Super Fiber Produced by the Gel Spinning of a Flexible Polymer," in *High-Performance and Specialty Fibers*, Tokyo: Springer Japan, 2016, pp. 109–132. doi: 10.1007/978-4-431-55203-1_7.

[59] Y. Xu *et al.*, "Nanostructured polymer films with metal-like thermal conductivity," *Nature Communications*, vol. 10, no. 1, pp. 1–8, 2019, doi: 10.1038/s41467-019-09697-7.

[60] S. Shen, A. Henry, J. Tong, R. Zheng, and G. Chen, "Polyethylene nanofibres with very high thermal conductivities," *Nature Nanotechnology*, vol. 5, no. 4, pp. 251–255, Apr. 2010, doi: 10.1038/nnano.2010.27.

[61] P. Smith and P. J. Lemstra, "Ultra-high-strength polyethylene filaments by solution spinning/drawing," vol. 15, pp. 505–514, 1980.

[62] D. B. Mergenthaler, M. Pietralla, H. G. Kilian, and S. Roy, "Thermal Conductivity in Ultraoriented Polyethylene," *Macromolecules*, vol. 25, no. 13, pp. 3500–3502, 1992, doi: 10.1021/ma00039a030.

[63] C. L. Choy, Y. Fei, and T. G. Xi, "Thermal conductivity of gel-spun polyethylene fibers," *Journal of Polymer Science Part B: Polymer Physics*, vol. 31, no. 3, pp. 365–370, 1993, doi: 10.1002/polb.1993.090310315.

[64] S. Ronca, T. Igarashi, G. Forte, and S. Rastogi, "Metallic-like thermal conductivity in a lightweight insulator: Solid-state processed Ultra High Molecular Weight Polyethylene tapes and films," *Polymer*, vol. 123, pp. 203–210, 2017, doi: 10.1016/j.polymer.2017.07.027.

[65] A. Henry and G. Chen, "High thermal conductivity of single polyethylene chains using molecular dynamics simulations," *Physical Review Letters*, vol. 101, no. 23, pp. 1–4, 2008, doi: 10.1103/PhysRevLett.101.235502.

[66] J. Gosumbonggot and G. Fujita, "Global maximum power point tracking under shading condition and hotspot detection algorithms for photovoltaic systems," *Energies*, vol. 12, no. 5, 2019, doi: 10.3390/en12050882.

[67] T. Takao *et al.*, “High thermal conduction bobbin and thermal stability of conduction cooled superconducting pancake coils,” *IEEE Transactions on Applied Superconductivity*, vol. 23, no. 3, 2013, doi: 10.1109/TASC.2013.2249552.

[68] G. Zerbi, G. Gallino, N. del Fanti, and L. Baini, “Structural depth profiling in polyethylene films by multiple internal reflection infra-red spectroscopy,” *Polymer*, vol. 30, no. 12, pp. 2324–2327, Dec. 1989, doi: 10.1016/0032-3861(89)90269-3.

[69] B. Bandeira, E. L. V. Lewis, D. C. Barton, and I. M. Ward, “The degree of crystalline orientation as a function of draw ratio in semicrystalline polymers: a new model based on the geometry of the crystalline chain slip mechanism,” *Journal of Materials Science*, vol. 51, no. 1, pp. 228–235, 2016, doi: 10.1007/s10853-015-9220-9.

[70] M. Hamzah *et al.*, “Surface chemistry changes and microstructure evaluation of low density nanocluster polyethylene under natural weathering: A spectroscopic investigation,” *Journal of Physics: Conference Series*, vol. 984, no. 1, 2018, doi: 10.1088/1742-6596/984/1/012010.

[71] P. Pagès, “Characterization of polymer materials using FT-IR and DSC techniques,” vol. 638, no. type V, pp. 121–140, 2005, [Online]. Available: http://ruc.udc.es/dspace/handle/2183/11499

[72] E. Agosti, G. Zerbi, and I. M. Ward, “Structure of the skin and core of ultradrawn polyethylene films by vibrational spectroscopy,” *Polymer*, vol. 33, no. 20, pp. 4219–4229, 1992, doi: 10.1016/0032-3861(92)90261-T.

[73] X. Wang, Q. Zhao, Z. Li, S. Yang, and J. Zhang, “Measurement of the thermophysical properties of self-suspended thin films based on steady-state thermography,” *Optics Express*, vol. 28, no. 10, p. 14560, 2020, doi: 10.1364/oe.392198.

Appendix A. FTIR spectrums of UHMWPE films

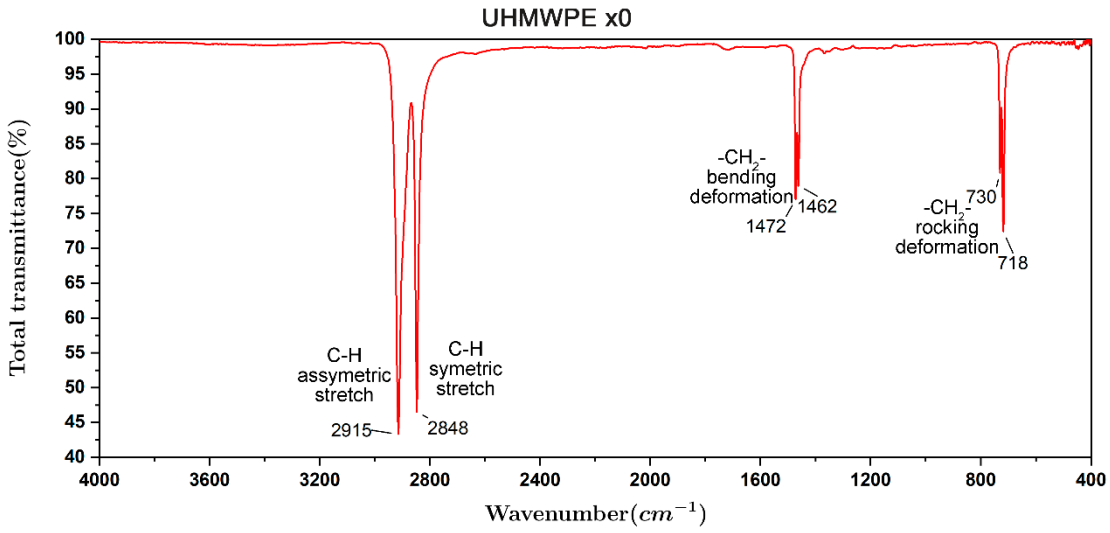

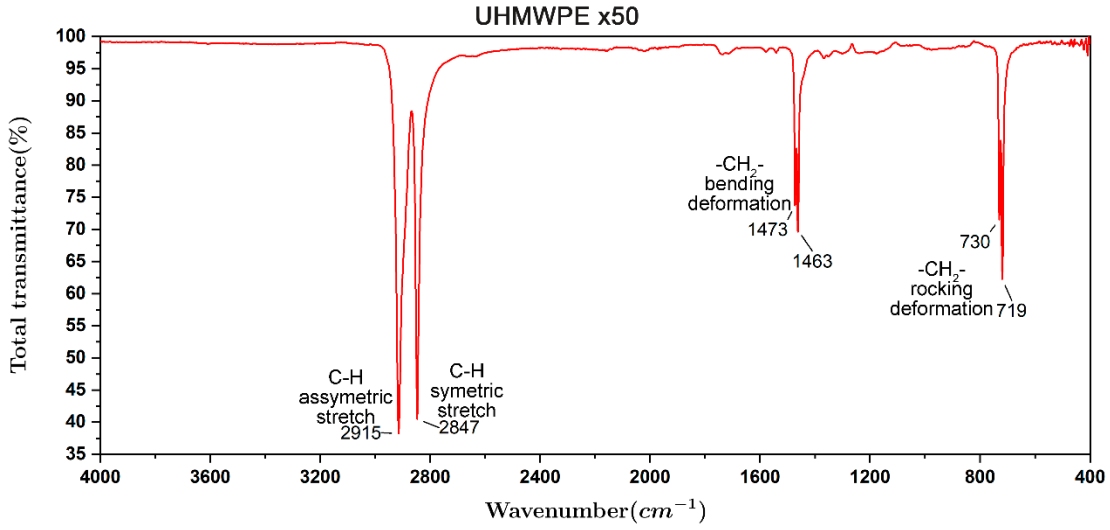

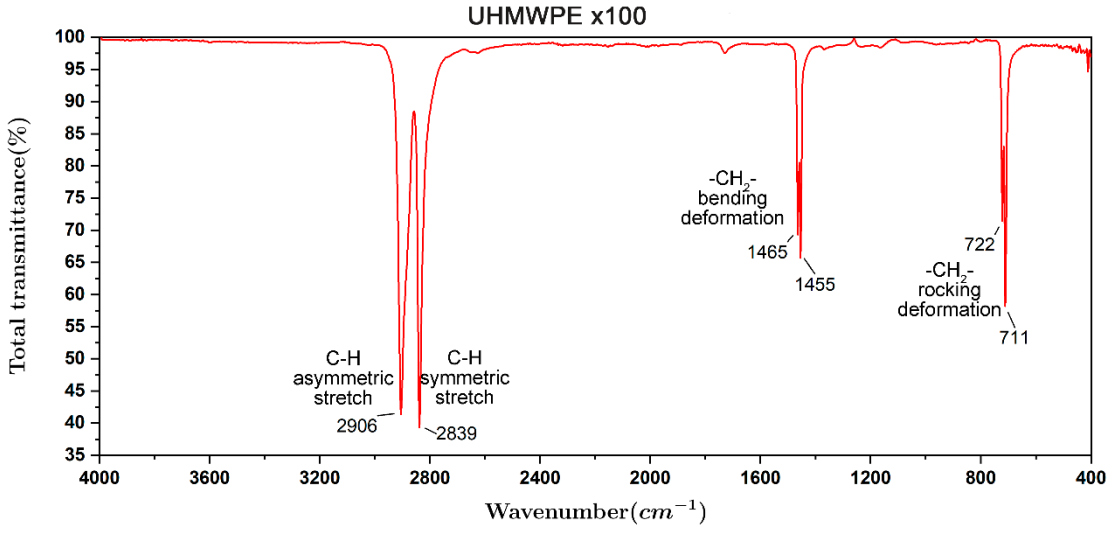

Appendix B. Scientific dissemination article published in TransferenciaTec Journal

Link to the article: https://transferencia.tec.mx/2020/10/06/los-termometros-infrarrojos-una-herramienta-inofensiva-y-util-en-la-nueva-normalidad/#:~:text=Inicio%20Destacado-,Los%20term%C3%B3metros%20infrarrojos%3A%20una%20herramienta%20inofensiva%20y%20%C3%BAtil%20en%20la,calor%20que%20emite%20nuestro%20cuerpo

Los termómetros infrarrojos: una herramienta inofensiva y útil en la nueva normalidad

Contrario a lo que se ha difundido por diversos medios, los termómetros infrarrojos ahora tan de moda, no ocasionan ningún tipo de daño en la salud, pues sólo miden el calor que emite nuestro cuerpo. Expertos te lo explican.

Por Eduardo Ramos, Alan Sustaita, y Marcelo Lozano

Con el comienzo de la denominada "nueva normalidad" provocada por la pandemia de COVID-19, es necesario seguir tomando medidas de prevención para controlar la propagación del virus. Una de ellas, y que ha causado mucha controversia, es el uso de termómetros infrarrojos para medir la temperatura corporal antes de ingresar a lugares públicos como supermercados, plazas comerciales, entre otros espacios cerrados de gran concurrencia. Como consecuencia del uso de estos dispositivos, se ha generado entre la población cierto temor derivado de la difusión de noticias falsas que aseguran que estos termómetros pueden ocasionar daños a la salud si la medición se realiza directamente en la frente o en la sien porque, supuestamente, emiten radiación que destruye las neuronas. Esta creencia es completamente falsa, porque los termómetros infrarrojos no emiten nada, pero entonces ¿Qué es esa luz que se ve en mi piel? Aquí se aborda el tema de manera simple y sencilla.

Cómo funcionan los termómetros

Un termómetro infrarrojo, también conocido como pirómetro, es un instrumento que es capaz de medir la temperatura de un objeto sin tocarlo, a partir de la medición del calor en forma de radiación que emite el objeto. Todo objeto emite calor en forma de radiación llamada infrarroja, de hecho, es una energía que no se puede ver, pero sí se puede sentir, coloca tu mano junto a una olla caliente y sentirás la radiación infrarroja. La configuración del termómetro convierte esa radiación en una señal eléctrica que se ajusta a ciertos valores

de calibración interna del mismo termómetro, para finalmente desplegar un valor de temperatura en la pantalla digital.

Existe una gran variedad de termómetros infrarrojos en el mercado, con los cuales, se apunta el termómetro hacia alguna pequeña zona de tu cuerpo, y el calor que emite esa zona de tu cuerpo entra al termómetro por un lente e inmediatamente te dice tu temperatura. Algunos termómetros, para facilitar la medición, tienen una luz o lámpara que ilumina la zona a donde vas a medir, del mismo modo que la mira telescópica de un rifle tiene un láser para saber a dónde estás apuntando, pero no te afecta en nada. Por eso algunos termómetros infrarrojos tienen una luz.

Todo cuerpo con masa emite energía en forma de radiación infrarroja, es decir, calor, la cual se genera por el movimiento de las partículas en su interior. El cuerpo humano emite radiación infrarroja debido a la actividad interna de los órganos provocando así una temperatura corporal promedio entre 36 y 37.5°C que se considera un rango normal. La radiación infrarroja que genera nuestro cuerpo contribuye a la sensación térmica que tenemos porque de cierta forma, la ropa que usamos atrapa y refleja de vuelta hacia el cuerpo todo este calor generado. ¿Te imaginas que pasaría si nuestra ropa dejará pasar este calor que emite nuestro cuerpo? Si esto ocurriera tendríamos una sensación de mayor frescura porque, en esencia, este calor sería liberado hacia el exterior. Imagínate, podríamos usar chamarra en la playa y no sentir calor.

Actualmente, en el Grupo de Investigación en Nanotecnología y Diseño de Dispositivos del Tec de Monterrey, estamos desarrollando un proyecto en conjunto con el MIT donde buscamos desarrollar fibras poliméricas sintéticas con esta propiedad de transparencia a la radiación infrarroja emitida por el cuerpo, para crear textiles avanzados. En la Figura 1 se puede apreciar el desempeño de este material. En ésta se ve que una película de dicho material cubre una parte de la mano que se expone a la visión de una cámara infrarroja. En la fotografía, y ante nuestros ojos, no se alcanza a apreciar el anillo que está situado justo debajo de la película. Sin embargo, la cámara infrarroja sí alcanza a ver lo que el lente de la cámara fotográfica y nuestros ojos no pueden ver, es decir, el anillo debajo de la película. Es como si la película de polímero que se observa de un color gris oscuro, no existiera para la cámara infrarroja. En otras palabras, la película es transparente a la radiación infrarroja.

A) B)

Figura 1. Desempeño de una película polimérica que es transparente a la radiación infrarroja. A) Imagen térmica en infrarrojo de una mano sin tela polimérica (se ve en la imagen la silueta del anillo). B) Imagen térmica en infrarrojo de una mano con una cinta de tela polimérica que es transparente a la radiación infrarroja (al calor, en la imagen no se ve la silueta de la cinta, pero sí la del anillo).

En la imagen de la izquierda, se puede ver el calor que emite la mano en infrarrojo, el anillo que cubre la piel genera una "sombra" del calor corporal en la imagen. En la imagen de la derecha, que está cubierta por una cinta de la tela polimérica transparente al calor que hemos desarrollado, se puede ver el anillo, igual que en la imagen de la izquierda, como si no estuviera la cinta de tela polimérica cubriendo la mano. Nuestros ojos no pueden ver el anillo que está situado justo debajo de la tela polimérica, sin embargo, la cámara infrarroja sí puede ver el anillo debajo de la tela. Es como sí la tela de polímero que se observa de un color gris oscuro, no existiera para la cámara infrarroja. En otras palabras, la cinta es transparente a la radiación infrarroja.

Si tuvieras puesta una camisa, una gorra o un cubre-bocas con esta tela, el termómetro infrarrojo podría medir tu temperatura sin quitártelo, porque podría "ver" a

través de la tela, ya que el calor en forma de radiación infrarroja la podría traspasar, y no estarías expuesto a ningún virus.

La radiación infrarroja

Pero ¿qué es la radiación infrarroja? La radiación infrarroja, o IR, es solo un tipo de radiación que existe en el espectro electromagnético (ver Figura 2). Otros tipos de radiación electromagnética incluyen las microondas (sí, las mismas que usa tu horno de microondas para calentar alimentos), los rayos X (exacto, esos que se usan en los equipos médicos para evaluar fracturas de huesos), y la luz visible. Ésta última es la única radiación que nosotros los seres humanos podemos detectar con nuestros ojos, y como se observa en la Figura 2, la luz visible corresponde solo a una porción muy pequeña de todo el espectro electromagnético.

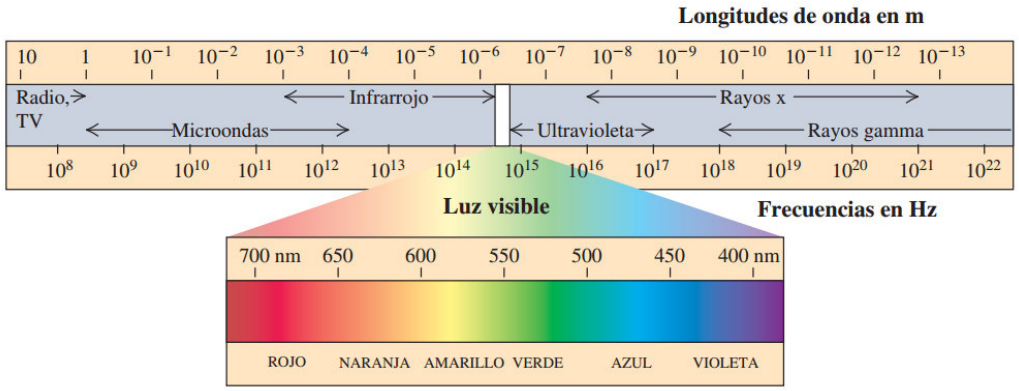

Figura 2. Espectro electromagnético.

Aunque nuestros ojos no pueden detectar la IR, seguramente podemos sentirlo porque como ya se mencionó anteriormente, la radiación IR es, literalmente, calor. Sitúate cerca de una chimenea o alrededor de una fogata, coloca tu mano cerca del carbón usado para preparar una rica carne asada aún y cuando la llama se haya extinguido, o camina en un clima frío bajo la luz del sol para sentir un poco de más calor. En todas estas experiencias, estás interactuando directamente con IR. Es este IR (calor) el que se puede medir.

La radiación IR funciona como la luz visible: puede enfocarse, reflejarse o absorberse. Por lo tanto, es válido hacer la analogía que un termómetro infrarrojo actúa hacia la radiación infrarroja de la misma manera que el ojo humano actúa hacia la luz visible. En este sentido, el ojo humano es un órgano que recibe los rayos luminosos procedentes de objetos y los transforma en impulsos eléctricos que son conducidos al centro nervioso de la visión en la parte posterior del cerebro, en donde son convertidos en imágenes. De manera análoga, el termómetro infrarrojo recibe la radiación infrarroja que emite tu cuerpo, y la

convierte en señales eléctricas para después convertirlo en un valor de temperatura. Como podrás ver, un termómetro infrarrojo, al igual que nuestros ojos, no emiten radiación alguna, solamente la reciben y enfocan o concentran la radiación infrarroja y visible, respectivamente, que provienen de otros objetos. Por eso no hay forma en que puedan causarte daño alguno.

Ahora que sabemos que nuestro cuerpo emite radiación infrarroja, es precisamente ésta la que se puede medir para detectar a personas que tengan fiebre, la cual es uno de los principales síntomas de la enfermedad provocada por el virus SARS-CoV-2, o COVID-19. Es por ello, que el mejor termómetro para usar en la "nueva normalidad" es el termómetro infrarrojo, que es una herramienta muy útil, además de ser inofensiva para el ser humano. Este tipo de termómetro ofrece una serie de ventajas que resultan bastante útiles para detectar personas posiblemente infectadas con el virus para este fin. La ventaja principal es que mide la temperatura corporal sin estar en contacto con la piel, reduciendo así los riesgos de transmisión del virus. Además, la temperatura se obtiene en cuestión de segundos. ¡Imagínate lo problemático que sería medir con un termómetro de otro tipo!

Errores al medir la temperatura

Sin embargo, algunos problemas surgen con el uso de estos dispositivos cuando no son empleados correctamente, lo que conlleva a obtener mediciones erróneas. Si te han medido la temperatura con este tipo de termómetros posiblemente te habrás dado cuenta de que se obtienen mediciones en un rango que puede ir desde 31 °C hasta 38 °C. Estos valores, evidentemente difieren mucho del rango de temperatura corporal normal de 36 °C – 37.5 °C, pero lo que es más grave es que cuando esto ocurre, en realidad el uso del termómetro no está cumpliendo su función de brindar seguridad de que una persona no tiene síntomas del COVID-19. Por eso siempre verifica que se te haga una correcta medición, preferiblemente en tu frente a una distancia de entre 3 y 5 cm, sin objetos ni maquillajes obstruyendo tu piel y en el interior de la puerta del lugar. Es parte de la "nueva cultura" y eso nos ayuda a todos.

Estos resultados erróneos se pueden deber a diversos factores que explicamos a continuación.

La precisión del termómetro IR se determina principalmente por la relación entre la distancia de medición y el tamaño del área del objeto a medir. En otras palabras, el área que se mide se hace más grande a medida que aumenta la distancia. Cuanto más pequeño sea el objetivo, más cerca deberías estar de él para realizar una medición (ver Figura 3). Por lo tanto, si te miden la temperatura con un termómetro IR apuntando a tu frente, pero el termómetro está a una distancia mayor a la que debería estar, podría estar también

midiendo la temperatura de tu pelo, por ejemplo, afectando el resultado pues el valor que despliega el termómetro equivale al promedio de temperatura de todo lo que el lente del termómetro alcanza a "ver". La recomendación de los fabricantes de los termómetros infrarrojos es tomar la temperatura directamente en la frente a una distancia de entre 3 a 5 centímetros, dependiendo del fabricante, por lo que, si se toman mediciones a mayores distancias o en otras partes del cuerpo el error de medición puede ser mayor.

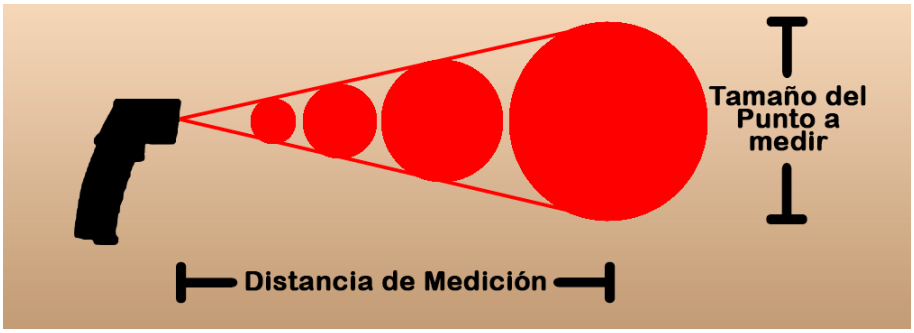

Figura 3. Rango de medición de un termómetro infrarrojo.

Otro factor que afecta la medición se presenta cuando el termómetro no está calibrado para medición de temperatura corporal. La base científica detrás del funcionamiento de un termómetro infrarrojo se conoce como Ley de Stefan-Boltzmann. Aunque la explicación de dicha Ley no la abordaremos en el presente artículo, sí es importante mencionar que esta ley emplea un concepto que toma mucha relevancia y que se conoce como emisividad. La emisividad es la radiación térmica emitida por un objeto debido a su temperatura en comparación con la que es emitida por un radiador perfecto a la misma temperatura. En otras palabras, representa la capacidad que tiene un cuerpo u objeto para irradiar calor. Como la emisividad es un valor que es comparado con la radiación emitida por un radiador perfecto, entonces toma valores entre 0 y 1, donde 1 es precisamente la emisividad de un radiador perfecto, también conocido como cuerpo negro. Así, un objeto con una emisividad de 0.9 emitirá el 90% y reflejará el 10% de la energía incidente. En general, cuanto mayor es la emisividad de un objeto, más fácil es para obtener una medición precisa de la temperatura usando un termómetro infrarrojo. Los objetos con emisividad por debajo de 0.2 pueden ser aplicaciones difíciles. De hecho, algunas superficies pulidas o metales brillantes como el aluminio reflejan tanto la radiación infrarroja que las mediciones de temperatura precisas no siempre son posibles.

El efecto de la emisividad puede explicarse de manera más clara usando la imagen de la Figura 4. Esta imagen fue obtenida con una cámara infrarroja. Una cámara infrarroja funciona con el mismo principio que un termómetro infrarrojo, con la ventaja que una cámara infrarroja puede desplegar una imagen con una escala de colores para poder distinguir diferentes temperaturas en la misma imagen. En principio, la mano y el anillo

deben estar a la misma temperatura debido al equilibrio térmico entre ambos. Sin embargo, de acuerdo con la escala de colores de la cámara termográfica, pareciera que el anillo está a una temperatura mucho menor que la mano. Esto se debe a que el metal refleja más radiación que la piel, es decir, tiene una emisividad mucho menor que la del cuerpo humano. Si la cámara está ajustada con el valor de emisividad del cuerpo humano, entonces generará un valor equivocado de la temperatura del anillo, y sucedería lo mismo si fuera al revés, es decir, si la cámara estuviera ajustada con el valor de emisividad del anillo dando una medición incorrecta de la temperatura de la mano.

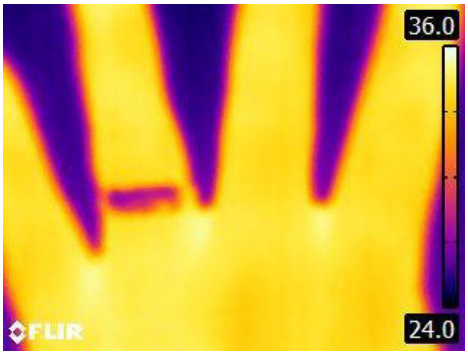

Figura 4. Imagen de una mano tomada con una cámara termográfica.

La emisividad del cuerpo humano es de 0.98, lo que representa otro aspecto favorable para el uso de termómetros infrarrojos de uso médico. Estos termómetros de infrarrojo de uso médico exclusivo en principio deben estar calibrados de acuerdo a la emisividad del cuerpo humano (0.98) y para un uso dentro de un rango de temperatura más acorde al del cuerpo humano (aproximadamente 20-60 °C) con un margen de error entre 0.1-0.5 °C. Por lo tanto, las mediciones suelen ser más precisas a que si se usará un termómetro infrarrojo de grado industrial, los cuales son empleados para una gran diversidad de materiales, cada uno con su propio valor de emisividad, y dentro de un rango muy amplio de temperatura que va desde temperaturas por debajo de 0°C hasta más de 1000°C.

Aún y cuando te midan la temperatura con un termómetro infrarrojo de uso médico exclusivo, todavía existe la posibilidad de que se obtengan medidas erróneas. Por ejemplo, si usas algún cosmético en el área del cuerpo donde se realiza la medición, esto podría modificar la reflexión de la piel, y por consiguiente la emisividad ya no sería 0.98, o incluso si estás sudando porque esto representa que hay otro material (en este caso un líquido) sobre la superficie. También, si la medición no se hace de manera perpendicular al área de medición, daría lugar a que solo una porción de la radiación emitida por el cuerpo humano llegue al lente del termómetro. Asimismo, si existe una corriente de aire al momento de la medición, o si ésta se realiza bajo la incidencia de los rayos del sol, o si el termómetro no está en equilibrio térmico con el ambiente donde se realiza la medición, la precisión del resultado también se vería afectada.

Conclusiones y recomendaciones

Ante la denominada “nueva normalidad” que ha surgido a raíz de la pandemia de COVID-19, los termómetros infrarrojos se han convertido en una herramienta tecnológica muy utilizada, y en muchos lugares indispensable, como parte de las acciones para tratar de controlar la expansión de la pandemia. Contrario a lo que se ha difundido por diversos medios, los termómetros infrarrojos representan una herramienta inofensiva para el ser humano ya que son dispositivos que únicamente reciben y enfocan la radiación infrarroja que emite nuestro cuerpo, para luego generar un valor de temperatura usando un sistema de calibración interno. Estos termómetros no emiten ningún tipo de radiación, por eso son seguros de usar con personas. Más aún, estos dispositivos resultan bastante útiles para detectar personas posiblemente infectadas con el virus SARS-CoV-2, considerando los riesgos propios de una pandemia, ya que algunas de sus principales ventajas son la medición de la temperatura corporal sin estar en contacto con la piel, reduciendo así el riesgo de transmisión del virus, y la obtención de resultados en cuestión de segundos, favoreciendo su uso en la entrada de lugares de gran concurrencia pública.

No obstante, existen numerosos factores que pueden afectar la precisión de los resultados generados. Por tal motivo, para obtener mayor precisión en los resultados, se sugiere tomar en cuenta las siguientes consideraciones:

- Dejar el termómetro infrarrojo en el ambiente de medición por lo menos 10 minutos antes de su uso. Esto para que el termómetro esté en equilibrio térmico con el ambiente.
- Confirmar que el área de la frente donde se realizará la medición está limpia, libre de cosméticos, y seca.
- Realizar la medición colocando el termómetro infrarrojo a una distancia dentro del rango recomendado por el fabricante.
- Realizar la medición colocando el termómetro de manera perpendicular a la superficie a medir, de preferencia en el área de la frente.
- Realizar la medición en un lugar libre de corrientes de aire, fuera de la luz del sol, es decir, en la sombra, y lejos de fuentes de calor.
- Asegurarse de que la temperatura de la frente no ha sido afectada por fuentes externas, por ejemplo, los rayos del sol (por eso es recomendable hacerlo en la sombra).

Ahora, ya sabes que usar un termómetro infrarrojo es totalmente seguro y puedes entrar con toda tranquilidad a cualquier lugar donde los utilicen como medida de seguridad.

Los autores

Jesús Eduardo Ramos Tirado es Ingeniero en Nanotecnología, egresado de la Universidad Politécnica de Sinaloa (2019). Es alumno de la Maestría en Nanotecnología del Tec de Monterrey, campus Monterrey. Trabaja en un proyecto con enfoque en polímeros para su potencial aplicación en textiles avanzados de control térmico personal.

Alan Osiris Sustaita Narváez es doctor en Ciencias, egresado de la Universidad Autónoma de San Luis Potosí (2007). Es profesor de la Escuela de Ingeniería y Ciencias en el Departamento de Mecánica y Materiales Avanzados del campus Monterrey, e investigador adscrito al Grupo de Investigación en Nanotecnología para el Diseño de Dispositivos. Es miembro del Sistema Nacional de Investigadores (nivel I).

Luis Marcelo Lozano Sánchez es doctor en Ciencias de Ingeniería, egresado del Tecnológico de Monterrey (2017). Es profesor en el Departamento de Ciencias del campus Guadalajara, e investigador adscrito al Grupo de Investigación en Nanotecnología para el Diseño de Dispositivos. Es miembro del Sistema Nacional de Investigadores (nivel I).

¿Quieres saber más?

Un material que se mantiene fresco y cool aún bajo el Sol
https://transferencia.tec.mx/2019/08/12/el-color-negro-nunca-fue-tan-fresco-y-cool/

"*Optical engineering of polymer materials and composites for simultaneous color and thermal management*"
https://www.scopus.com/record/display.uri?eid=2-s2.0-85065831199&doi=10.1364%2fOME.9.001990&origin=inward&txGid=29baec4dc46520a2a457e77bf90739f5